

The BIOMASP+ project on biosphere-atmosphere exchanges and their role in air pollution in the subtropical megacity of São Paulo: motivations, methods and preliminary observations

Agnès Borbon^a, Adalgiza Fornaro^b, Amauri P. Oliveira^b, Silvia R. Souza^c, Joël P. de Brito^d, Jean-Luc Jaffrezo^e, Michael Staudt^f, Rita Y. Ynoue^b, Georgia Codato^b, Maciel P. Sánchez^b, Lucas C. Silveira^b, Luciana Rizzo^g, Fernanda Anselmo-Moreira^c, Etienne Brugère^a, Pauline Fombelle^a, Manon Rocco^{b,p}, Leonardo Domingues^{b,q}, Samara Carbone^h, Eduardo L. M. Catharino^c, Aurélie Colomb^a, Jacques Florêncio^o, A. Gandolfoⁱ, Marina Jamaral^d, J. Kempf^f, Alex Nascimento^c, Olatunde Murana^d, Jean-Eudes Petitⁱ, Daniel C. Zacharias^r, Junteng Wu^a, Alexandre Albinet^l, Hugo H. Araújo^l, Jean-Luc Baray^a, Marie Bertrand^a, Maria L. A. M. Campos^o, Lucas Chiari^b, Armelle Crouzet^c, Pamela A. Dominutti^c, Sébastien Dusanter^s, Cláudia Maria Furlan^k, Bruno Ruiz Brandão da Costa^k, Morgan Lopezⁱ, Jean Martins^c, Tarcisio F. Martins^c, Kátia Mazzei^c, Camila S. Meireles^l, Gregori A. Moreira^{m,r}, Eduardo Landulfo^m, Edson P. Marques Filhoⁿ, Michel Ramonetⁱ, Véronique Riffault^d, Ávila B. Santos^b, Bruna L. Paim^b, Luzimar C. Silva^l, Graciele D. D. Soares^l, Gaëlle Uzu^c, Weixin Xian^a

Affiliations: ^a Univ. Clermont Auvergne, CNRS, LaMP, OPGC, Clermont-Ferrand, France; ^b Dept. Ciências Atmosféricas, Instituto de Astronomia, Geofísica e Ciências Atmosféricas, Univ. São Paulo (IAG-USP), Brazil; ^c Núcleo de Uso Sustentável dos Recursos Naturais, Instituto de Pesquisas Ambientais (IPA-SP), São Paulo, Brazil; ^d IMT Nord Europe, Institut Mines-Télécom, Univ. Lille, Centre for Energy and Environment, 59000, Lille, France; ^e Univ. Grenoble Alpes, CNRS, INRAE, IRD, Grenoble INP, IGE, 38000 Grenoble, France; ^f CEFÉ, CNRS, EPHE, IRD, Univ Montpellier, Montpellier, France; ^g Instituto de Física (IF-USP), Brazil; ^h Universidade Federal de Uberlândia (UFU), Brazil; ⁱ Laboratoire des Sciences du Climat et de l'Environnement, CEA, CNRS, Gif sur Yvette, France; ^j Institut National de l'Environnement Industriel et des Risques (INERIS), Verneuil-en-Halatte, France; ^k Instituto de Biociências (IB-USP), Brazil; ^l Universidade Federal de Viçosa (UFV), Brazil; ^m Instituto de Pesquisas Energéticas e Nucleares (IPEN), Brazil; ⁿ Universidade Federal da Bahia (UFBA), Brazil; ^o Dept. Química, Faculdade de Filosofia, Ciências e Letras de Ribeirão Preto (FFCLRP-USP), Brazil; ^p Now at Aix Marseille Univ., CNRS, LCE, Marseille, France and CNRS, Aix Marseille Univ, IRD, Avignon Univ, IMBE, Marseille, France; ^q Instituto de Recursos Naturais, Universidade Federal de Itajubá (UNIFEI), Itajubá, Brazil; ^r Instituto Federal de São Paulo (IFSP), Registro, São Paulo, Brazil.

Corresponding authors: Agnes Borbon agnes.borbon@uca.fr / Adalgiza Fornaro adalgiza.fornaro@iag.usp.br

Abstract

Air pollution, especially in urban areas, is the result of a complex mixture of natural and anthropogenic emissions and their atmospheric processing. It causes millions of premature deaths worldwide and affects plant metabolism, which in turn alters the emissions of Biogenic Volatile Organic Compound (BVOCs) by plants. By taking the subtropical Metropolitan Area of São Paulo (MASP) as a natural laboratory, the BIOMASP+ project (BIOsphere-atmosphere

Early Online Release: This preliminary version has been accepted for publication in *Bulletin of the American Meteorological Society*, may be fully cited, and has been assigned DOI 10.1175/BAMS-D-23-0161.1. The final typeset copyedited article will replace the EOR at the above DOI when it is published.

© 2025 American Meteorological Society. This is an Author Accepted Manuscript distributed under the terms of the default AMS reuse license. For information regarding reuse and general copyright information, consult the AMS Copyright Policy (www.ametsoc.org/PUBSReuseLicenses).

interactions in the Metropolitan Area of São Paulo - *plus*) aims to evaluate the interplay between the biosphere and secondary pollution (ozone and SOA formation and aging). The Brazilian Atlantic Forest (Mata Atlântica) is the target ecosystem as the fifth biodiversity hotspot in the world. Here we present the scientific motivations of the project, its methodology and the preliminary observations from the Special Observation Periods of year 2023 (SOP1, 2, 3 and 4). BIOMASP+ is (i) integrative, by combining in-situ/remote/laboratory observations and modeling, (ii) multidisciplinary, addressing micrometeorology, urban climate, atmospheric chemistry and biology. The project involves multiple nested scales: from leaf to above-canopy levels, from very short time (microseconds) to multi-year scale, from few millimeters (turbulence scale) to synoptic scale. In particular, the experimental effort relies on the implementation of two contrasting supersites (primary forest and urban forest) with a 30-m and 20-m flux towers, respectively, and a variety of state-of-the-art instruments. Ambient observations and the quantification of BVOC emissions have highlighted the complex interactions between meteorology, atmospheric composition of pollution, biogenic emissions of representative remnants of the Atlantic Forest and anthropogenic emissions.

Capsule

Since 2022, the international and multidisciplinary BIOMASP+ project has been addressing meteorology, matter fluxes, atmospheric chemistry of reactive species (gases and aerosols), and biology through comprehensive experimental efforts in the megacity of São Paulo.

Significant statement

The purpose of the BIOMASP+ project is to understand the interactions between the biosphere and urban pollution in a multidisciplinary way. It is an important topic in an era of decarbonization and a warming climate expected to enhance emissions from the vegetation. The project is based on an experimental effort in the subtropical megacity of São Paulo, Brazil, combining state-of-the-art instrumentation for gas and particle properties, biogenic emission chambers, a photochemical reactor and micrometeorology flux towers. The Special Observation Period (SOP) of April-July 2023 confirmed the complex coupling between air pollution and meteorology and the combined effect of both anthropogenic and biogenic emissions on the atmospheric composition, even in the surrounding forested areas.

Biosphere–atmosphere interactions and urban pollution

Urban air pollution arises from a complex mixture of primary compounds originating from both natural sources, such as biogenic volatile organic compounds (BVOCs), and anthropogenic emissions, including anthropogenic volatile organic compounds (AVOCs), nitrogen oxides ($\text{NO}_x = \text{NO} + \text{NO}_2$), carbon monoxide (CO) and primary particulate matter. Through complex mechanisms under suitable meteorological conditions and photochemical reactions, these compounds produce secondary pollutants such as ozone (O_3) and secondary organic aerosols (SOA). These pollutants contribute to millions of premature deaths worldwide (WHO 2021) and negatively impact plant metabolism and natural ecosystems (Stevens et al. 2020). Moreover, SOA plays a critical role in the Earth's radiative balance, representing one of the largest uncertainties in climate models (Tsigaridis and Kanakidou 2018). Under conditions of lower NO_x , economic decarbonization efforts, and climate warming, BVOC emissions from urban vegetation may increase. As a consequence, the formation of O_3 and SOA may become even more sensitive to these BVOC emissions (Liaskoni et al. 2024; Gao et al. 2022; Penuelas and Staudt 2010).

The mechanisms of ozone production from biosphere-atmosphere interactions were first elucidated in Atlanta by Chameides et al. (1988) and have been extensively studied since then (Fitzky et al. 2019; Fierravanti et al. 2017; Calfapietra et al. 2013). The processes of SOA formation from these interactions have also been intensively investigated (Li et al. 2022; Takeuchi et al. 2022; Voliotis et al. 2022; Xu et al. 2021; McFiggans et al. 2019; Srivastava et al. 2017; Xu et al. 2015; Shillings et al. 2013; Carlton et al. 2009; Hallquist et al. 2009). BVOCs, primarily unsaturated hydrocarbons such as isoprene (2-methyl-1,3-butadiene), monoterpenes, and sesquiterpenes, can undergo oxidation reactions with the three main oxidants (OH, ozone and NO_3), leading to the formation of ozone and SOA. SOA yields significantly vary among BVOC from one to three orders of magnitudes as reported by Farhat et al. (2025). The contribution to SOA formation also depends on ambient conditions such as NO_x levels, temperature and organic aerosol concentrations. Under high NO_x conditions, AVOCs such as toluene can exhibit SOA yields on the order of 10% (Ng et al. 2007), whereas isoprene under similar conditions exhibit yields three times lower (Kroll et al. 2006). However, large heterogeneity in ambient conditions in terms of NO_x , temperature, organic aerosol loads - including within urban areas - can lead to substantial variation in SOA formation mechanisms and yields (Srivastava et al. 2022; Wennberg et al. 2018). Notably, the oxidation products of BVOCs, mainly semi-volatile compounds, exhibit higher yields in SOA production compared

to those of anthropogenic origin. Quantification of semi-volatile species and their partitioning between the gas and particulate phases is essential for a deeper understanding of SOA formation and its dependence on anthropogenic NO_x levels (Voliotis et al. 2022b; Heald and Kroll 2020; Donahue et al. 2006). Recent studies have highlighted the biogenic component of urban pollution. Therefore, it is urgent to consider BVOC emissions to accurately assess their potential for O₃ and SOA production and, consequently, their impacts on health (Déméautis et al. 2022) and climate (Dominutti et al. 2024; Fitzky et al. 2019; Ren et al. 2017). The complexity of this issue is compounded by the fact that BVOC emissions, both in terms of quantity and composition, vary significantly among plant species and are strongly influenced by environmental factors such as air pollutants, UV radiation, temperature, soil water availability, and seasonal variations (Fierravanti et al. 2017).

Despite the long-recognized importance of biosphere-atmosphere interactions in urban pollution, our understanding remains incomplete in large metropolitan areas given the strong heterogeneity of AVOC and BVOC presence, the large heterogeneity in their ozone and SOA forming potentials, the emerging importance of the anthropogenic nature of terpenoids (Peron et al. 2024; Borbon et al. 2023; Gu et al. 2021; Churkina et al. 2017) and the heterogeneity of ambient conditions. The differences between these emissions and the potential for O₃ and SOA formation, as well as the photochemical reactions involved in these processes, may be especially important in poorly explored ecosystems, such as the Atlantic Forest in Brazil (Santos et al. 2022).

In this context, the BIOMASP+ project addresses the role of biosphere-atmosphere interactions in urban pollution, by considering its physicochemical and biological dimensions from both emission and atmospheric chemistry perspectives. BIOMASP+ builds upon two previous initiatives. The first, MCITY Brazil, has involved continuous turbulent flux measurements at urban, suburban and rural locations in MASP since 2013, providing critical insights into the surface energy and radiation budget, local circulation patterns, the urban heat island effect, and boundary layer characteristics (Ferreira et al. 2024; Oliveira et al. 2020). The second project, BIOMASP: Biosphere-atmosphere interactions in the São Paulo Metropolitan Area (Brazil-France collaboration), provided the first data on atmospheric isoprene concentrations from representative sites of the Atlantic Forest, within and outside the densely urbanized area of MASP, in 2018 and 2019 (Santos et al. 2022).

The Metropolitan Area of São Paulo (MASP): a paradigm for the study of atmospheric biogenic-anthropogenic interactions

The Atlantic Forest (Mata Atlântica): an island within the sea of human-made disturbances

The Atlantic Forest is the most densely populated biome in Brazil, home to about 70% of the Brazilian population, although it covers only about 15% of the country's territory (Fundação SOS Mata Atlântica; INPE 2023). The Southeast region encompasses a substantial part of the preserved biome (around 40%) but is under high pressure due to its increasing urbanization, such as the Metropolitan Area of São Paulo, and its economy, which is heavily based on agriculture and livestock. The native Atlantic Forest cover, found in small to large forest fragments, has continued to decrease in the last decade, with deforestation rates ranging from approximately 11,400 to 29,000 ha/year (Fundação SOS Mata Atlântica; INPE 2023), despite Law no. 11,428/2006 – known as the Atlantic Forest Law – which deals with the conservation, protection, and regeneration of the biome. This deforestation even affects old native forests, which are responsible for irreplaceable ecosystem services and biodiversity conservation. In fact, there is an ongoing progressive process of rejuvenation of the Atlantic Forest, especially in flatter areas (Rosa et al. 2021). Forest fragments have not only lost biomass but also biodiversity, with species loss rates ranging from 23% to 31% over the last 40 years (Lima et al. 2020).

MASP: Air pollutants and climatology

MASP is one of the world's largest megacities, with a population exceeding 20 million and a fleet of approximately 7 million vehicles (CETESB 2024). This fleet burns a complex mix of fuels. Consumers can choose between gasoline with 27% ethanol content and anhydrous ethanol (both for flex-fuel passenger vehicles) (Frutuso et al. 2023). Buses and trucks use diesel-S10 (blended with 10% biodiesel). According to the official emissions inventory of the Environmental Agency of São Paulo State (CETESB), fuel combustion from the vehicle fleet accounts for more than 90% of carbon monoxide (CO) emissions, 70% of hydrocarbons (HC), 60% of NO_x, 40% of particulate matter (PM₁₀), and 8% of sulfur oxides (SO_x) (CETESB 2024). The total annual mass emissions (1000 t / year) decreased substantially between 1994 and 2023, by more than 6, 12, 17, 19 and 20 times for NO_x, HC, CO, SO₂ and PM₁₀, respectively (CETESB 2024). This progress in reducing pollutant emissions can be largely attributed to the establishment of the Brazilian Air Pollution Control Program for Motor Vehicles

(PROCONVE) in 1986, despite a more than eightfold increase in the number of vehicles over the past five decades (CETESB 2024; Fornaro and Gutz 2006; CETESB 1994). Thus, significant improvements in air quality were observed between 1994 and 2023. PM₁₀ concentrations decreased from 70 to 27 $\mu\text{g}\cdot\text{m}^{-3}$ on an annual average while PM_{2.5} levels remained relatively stable at 15 $\mu\text{g}\cdot\text{m}^{-3}$ over the last 12 years. The official inventory estimates that 50% of PM_{2.5} production originates from secondary atmospheric reactions. Such absence in the PM_{2.5} trend raises the role of BVOC precursors in its secondary formation. Carbon monoxide (CO) levels also showed a notable reduction, declining from 6 ppm to less than 1 ppm over the same period (CETESB 2024). Despite the reduction in its precursor emissions, ozone concentrations remain stable, as illustrated in Figure 1. While NO_x precursor concentrations have decreased significantly over the last 20 years (Fig. 1), ozone concentrations have increased slightly, indicating the well-known NO_x-saturated regime in MASP (Schuch et al. 2019; Orlando et al. 2010). As for PM_{2.5}, the temporal evolution of ozone also raises the role of BVOC precursors in its formation. The emissions of BVOC precursors are expected to increase in the regional warming climate of MASP observed over the last two decades (see next section).

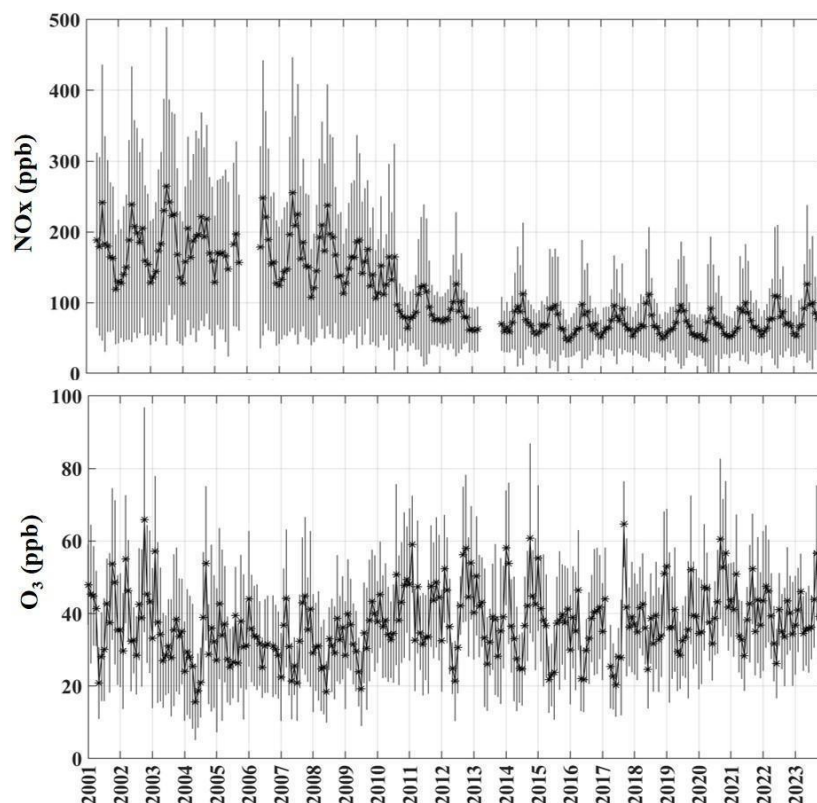


FIG. 1. Trends in monthly averages of hourly NO_x mixing ratios (Congonhas Air Quality Station) and daily 8-hour maximum O₃ mixing ratios (Ibirapuera Air Quality Station), along with their standard deviations, based on data from the official air quality monitoring network, from May 2001 to April 2024 (CETESB, QUALAR). The distance between these two stations is 4.5 km.

The climate of the MASP is classified as high-altitude subtropical humid, characterized by dry and mildly cold winters (June–August) and wet and warm summers (December–February) (Alvares et al. 2013). These seasonal variations are influenced by the altitude of the region (~750 m) and its proximity to the Atlantic Ocean (~55 km; see Fig. SM1 and Table SM1). The seasonal pattern of meteorological conditions in MASP is controlled by the position and intensity of the semi-permanent South Atlantic subtropical high and continental low-pressure systems. This large-scale pattern is often perturbed by the passage of cold fronts throughout the year (Sánchez et al. 2020). In addition, MASP is influenced by meso- and local-scale circulations such as Sea Breeze (SB), mountain-valley flows, and UHI (Urban Heat Island) circulations (Oliveira et al. 2020; Ribeiro et al. 2018). These thermally induced circulations arise from horizontal thermal contrasts induced by differences in land-ocean thermal capacity, topography, and land use configuration of the MASP (Ferreira et al. 2024; Moreira et al. 2022a; Moreira et al. 2022b; Sánchez et al. 2022; Silveira et al. 2022; Oliveira et al. 2020; Sánchez et al. 2020; Ribeiro et al. 2018).

During the two 30-year normal periods (1961–1990 and 1991–2020), MASP exhibited a consistent increase in temperature (Fig. SM2a, Table SM2) and summer rainfall (Fig. SM2c, Table SM2), with a concomitant decrease in relative humidity (Fig. SM2b, Table SM2) and wind speed (Fig. SM2d, Table SM2). These changes are attributed to the combined effects of urbanization (e.g., vertical expansion of buildings and increasing the impermeability of surfaces) and global climate change (Oliveira et al. 2020; Marengo et al. 2018). The UHI also exhibits strong gradients, and its effects are more pronounced in areas further from the Atlantic Ocean (Fig. SM3 and Table SM2). The subtropical climate, with a dry period in winter and hot and rainy summers (Fig. SM2), presents a high potential for intense biogenic emissions in spring and summer in MASP (Santos et al. 2022). All together, these climatological conditions are favorable to photochemical activity, and, as a consequence, a production of O₃ and SOA can be expected.

Objectives of the BIOMASP+ project

The Franco-Brazilian BIOMASP+ project uses the MASP region as a natural laboratory to fill critical gaps in the understanding of atmospheric processes influenced by anthropogenic and biogenic emissions. This area, with remnants of the Atlantic Forest, provides a unique urban ecosystem to study. Using a multidisciplinary approach, the BIOMASP+ consortium investigates the interactions between the biosphere, air quality, climate, and human health under changing climate conditions. The study addresses the following key scientific questions:

- How do biosphere-atmosphere interactions affect secondary pollution (ozone formation, SOA production and aging) and health?
- What are the feedbacks of these interactions on the biosphere?

Methodology

The methodology in BIOMASP+ combines in-situ observations, laboratory experiments, 0D box modeling and 3D modeling with the Weather Research and Forecasting coupled to the Chemistry (WRF-Chem) model (Grell et al. 2005) and the Model of Emissions of Gases and Aerosols from Nature (MEGAN - Guenther et al. 2006). The project is divided into four tasks (see SM for a full description of each task). The experimental design includes several observation periods to describe and quantify in detail the meteorology and the dynamics (surface, mixing and entrainment layers during the convective regime within the urban roughness and role of topography), the properties of gases and aerosols (physics, chemical composition, reactivity and oxidative potential), and the emissions of BVOCs thanks to state-of-the-art instrumentation (Table SM4a, SM4b, SM4c and SM4d). Five Special Observation Periods (SOP1 to SOP5) have been implemented for an in-depth analysis of BVOC emission fluxes and biophysical-chemical processes, as well as two Extended Observation Periods (EOP) of at least one year to enable a long-term integration of meteorological conditions, emission dynamics, atmospheric concentrations, and chemical transformations (EOP1 and EOP2) (Table SM3). 0-D box physico-chemical modeling and 3D modeling will be constrained by observations collected during SOPs for an in-depth investigation of the atmospheric processing of gases and particles and an evaluation of air quality changes in MASP regarding the interactions with the Atlantic Forest emissions at present and under changing climate conditions (see Task 4 in the SM).

The experimental effort focused on field campaigns conducted at two contrasting sites (Fig. 2). The first site, Matão-IAG on the University of São Paulo campus (USP, 23°33'34"S; 46°44'01"W; 744 m asl), is located in a densely urbanized area and is affected by both biogenic emissions from nearby urban forests and anthropogenic pollution from the MASP. The second site, Morro Grande Reserve (RMG) (23°39'15"S; 46°58'9"W; 890 m asl), is expected to be predominantly influenced by biogenic emissions from the Atlantic Forest (Fig. 2). The 30-m tower and a shelter at its base were installed at the RMG site (Fig. 2c and 2d), and the 20-m tower was set up at the top (17 m high) of the main IAG building at the Matão-IAG site (Fig. 2e and 3). Conventional meteorological and flux (CO_2 , H_2O and energy) instruments were implemented at the end of 2022. In 2023, during the wet-transition and dry seasons, SOPs 1, 2, 3 and 4 investigated BVOC emissions and biophysicochemical atmospheric processes. For the latter, the experimental design at the two supersites (inlets and instrumentation) is shown in Figure 3. At the RMG site, a trailer 200 m away from the tower was also deployed for additional observations (Fig. 3). To complement the field experiments, laboratory experiments dedicated to the quantification of BVOC emissions were performed at the Environmental Research Institute (IPA-SP), using standard biogenic emission and fumigation chambers (Fig. 2f), a greenhouse chamber for species cultivation and acclimation (Fig. 2j and 2k), and analytical devices (see Task 2 and Instrumentation sections in SM).

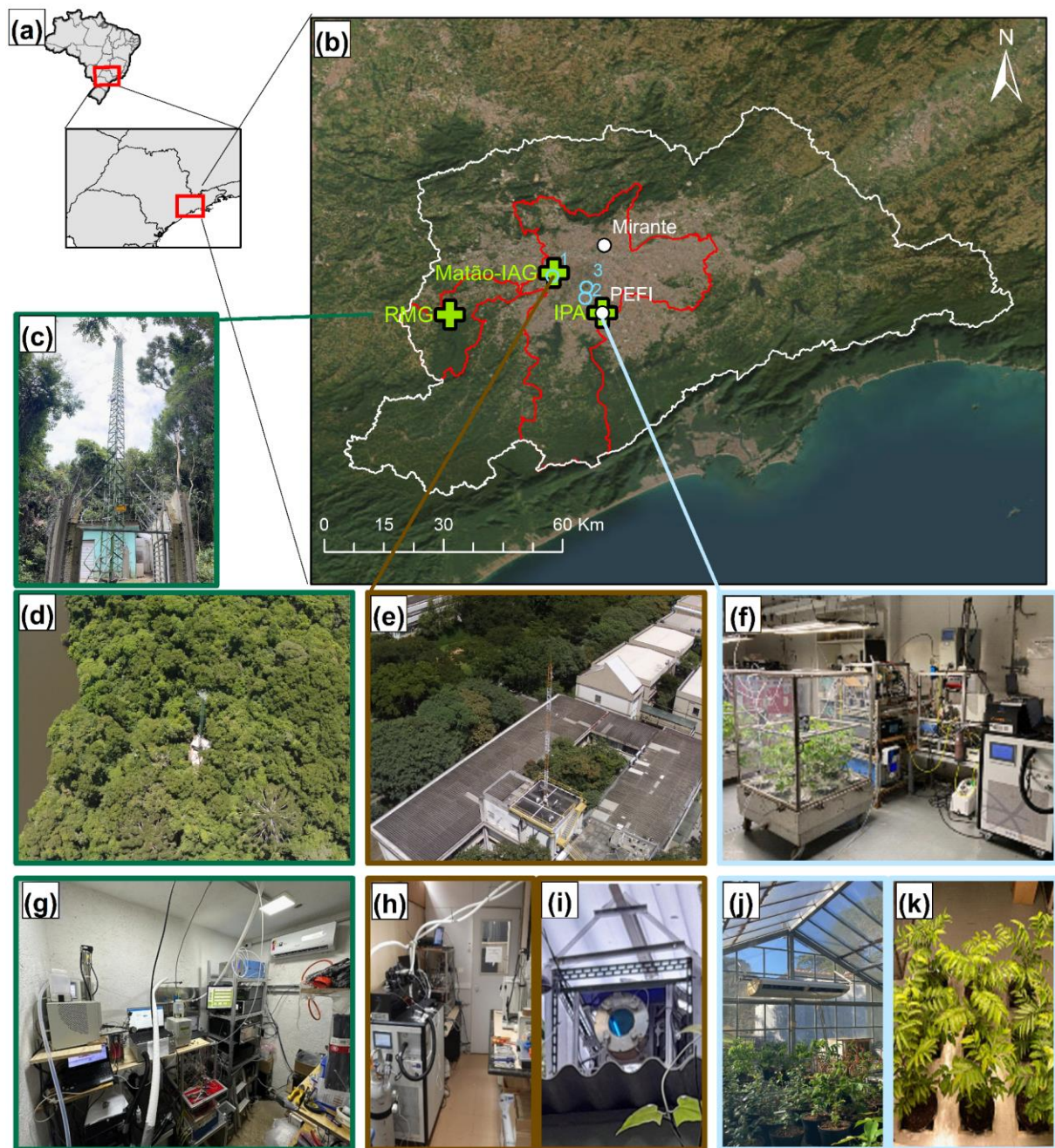


FIG. 2. The experimental set-up of BIOMASP+ within the Metropolitan Area of São Paulo (MASP): a) Maps of Brazil and São Paulo State, b) Satellite image of MASP (in white) and the cities of São Paulo and Cotia (in red), where the Matão-IAG and RMG supersites are located. Pictures: c) Tower and shelter at RMG, d) View of the top of the RMG tower by drone, e) View of the top of the Matão-IAG tower by drone, f) Fumigation chambers and instruments at IPA-SP, g) Instruments inside the RMG shelter, h) Instruments in the Matão-IAG laboratory, i) Potential Aerosol Mass-Oxidation Flow Reactor (PAM-OFR), j) Greenhouse at IPA-SP, and k) Some species for chamber studies at IPA-SP.

To evaluate the regional representativeness of the observations within the MASP domain and to put them into a historical perspective, the project also benefits from the ongoing observations performed by the meteorological and air quality networks on the ground. Climatological and meteorological data have been obtained from the MIRANTE and PEFI stations (Fig. SM1, Table SM1 and SM2). Atmospheric pollutants (O_3 , NO_x , CO, SO_2 , $PM_{2.5}$ and PM_{10}) have been monitored since the 1980s by the official network (data accessible in the Qualar-CETESB system) with more than 15 stations in MASP (CETESB 2024). Since March 2024, three new low-cost pollutant sensors (Vaisala AQT530, Petäjä et al. 2021) have been installed at the BIOMASP+ sites (RMG, at two different heights: 12 m and 31 m) and Matão-IAG (10 m).

To extend the spatial scale of the in-situ observations by considering the atmosphere in its three dimensions, remote sensing and sounding free balloon observations complement the ground-based measurements. The daytime variation of the urban planetary boundary layer (PBL) is evaluated by LIDAR installed at the *Instituto de Pesquisas Energéticas e Nucleares* (IPEN-USP) in the same area of the Matão-IAG site (Fig. 2 and Fig. SM1). The BIOMASP+ project will provide an opportunity, similar to the previous analysis, to conduct a 10-day observation campaign in 2026, with launched rawinsondes, including O_3 vertical profiles, every 3 hours at the RMG site, a rural forested area within MASP (Sánchez et al. 2025). Formaldehyde columns obtained by the TROPOMI-Sentinel satellite (Freitas and Fornaro 2022) are also part of the BIOMASP+ scope dataset, and for this compound in particular, surface measurements with Differential Optical Absorption Spectroscopy (DOAS) are scheduled to start in August 2025. Together with in-situ air quality observations from the air quality network, these observations are useful to constrain the WRF-Chem model outputs.

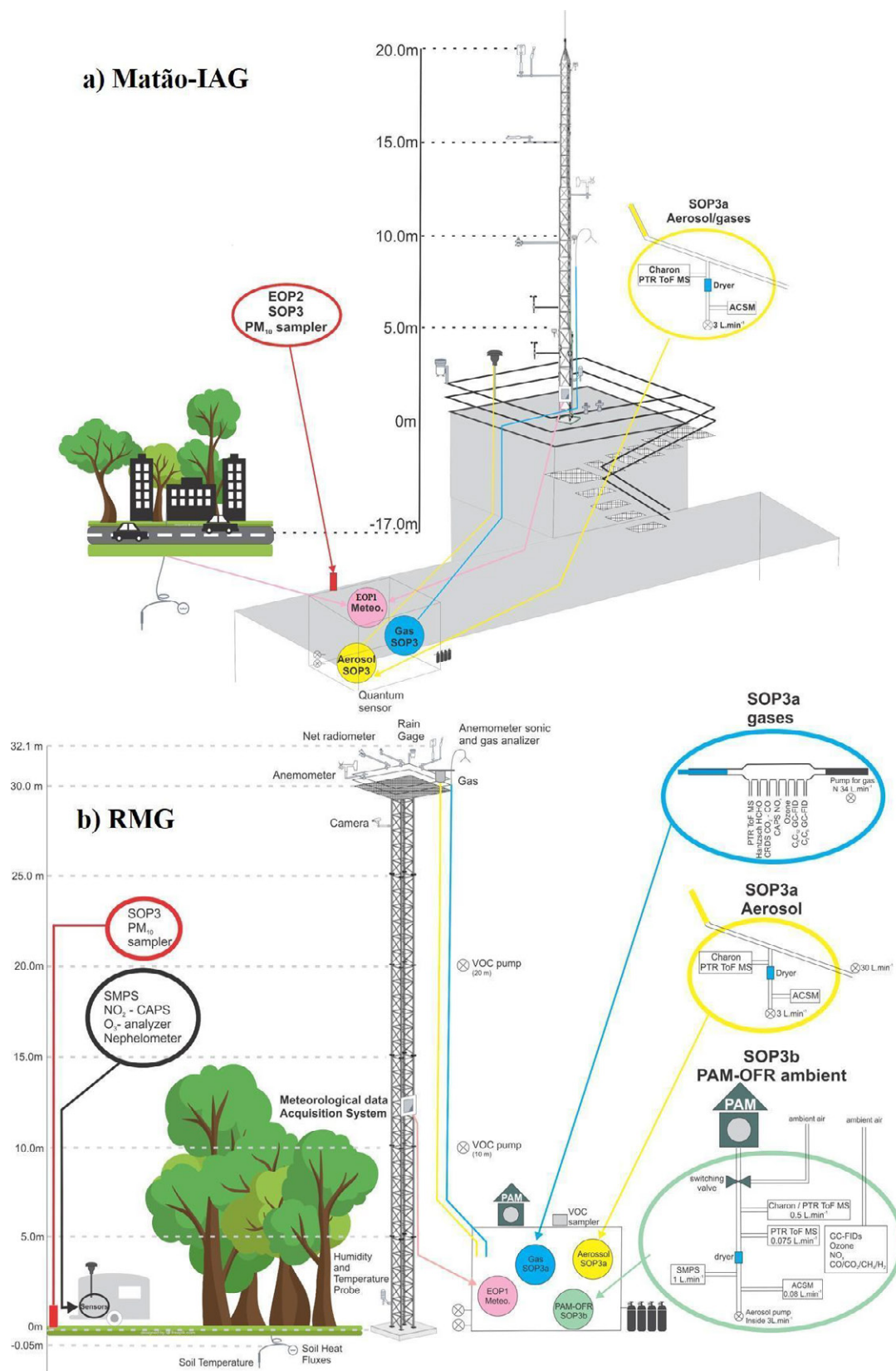


FIG. 3. Diagram of the Matão-IAG (20 m high from a platform at the top of one of the IAG-USP buildings) and RMG (30 m high from the ground) towers, showing the main infrastructure and

instruments for extensive (EOP) and intensive (SOP) observation periods. Instrumentation is detailed from Table SM4a to Table SM4d in the SM.

The Special Observation Periods of 2023

During the year 2023, four SOPs were implemented to characterize BVOC emissions of representative remnant species of the Atlantic Forest, the properties of gases and aerosols and the meteorology at the two contrasting sites. These preliminary observations are the basis of future analysis within BIOMASP+.

First insights into floristic diversity, BVOC emissions and leaf anatomy in response to urban stress during SOP1 and SOP2

In the floristic survey of the Matão-IAG forest, 194 individuals of 48 species from 20 families were characterized (Fig. SM7). The tree density was 970 individuals ha⁻¹ and the mean cross-sectional area of tree trunks was 5.19 m² ha⁻¹. Of the 48 documented species, 54% belonged to the families Myrtaceae, Lauraceae, and Euphorbiaceae. The most dominant species were the Euphorbiaceae *Croton floribundus* and *Alchornea sidifolia*, which together accounted for 31.3 % of the floristic composition and also reached the highest cover values (Fig. SM7). 25 species (52%) were native to Brazil, of which 19 (39.6%) were endemic (mainly Lauraceae and Myrtaceae). Two species, *Coffea arabica* and *Archontophoenix cunninghamiana*, were classified as exotic. Several species, including *Eugenia pruinosa* and *Ocotea odorifera*, are listed as endangered or threatened (MMA 2022).

In the RMG forest, 188 individuals belonging to 43 species of 22 families were identified (Fig. SM7). The tree density of 940 individuals/ha was similar to that of the Matão-IAG site, while the average cross-sectional area of tree trunk was higher at 8.75 m² ha⁻¹. The main families were Fabaceae, Meliaceae and Sapindaceae. Among the endemic species, *Ocotea glaziovii* had the highest number of individuals. *Nectandra barbellata* and *Ocotea odorifera* were listed as endangered and *Araucaria angustifolia* as critically endangered (MMA 2022). *Pittosporum undulatum* was designated as exotic. The average LAI in the RMG forest was 5.3 ± 0.3.

Comparison of four selected species growing in both sites suggests that vegetation in the RMG is less affected by urban stress than vegetation in Matão-IAG (Fig. 4Aa-4Ah). Visually, all plants in the Matão-IAG presented higher levels of visual leaf damage compared to RMG plants (Fig. 4Aa-4Ab). The leaves of the Matão-IAG species showed larger chlorotic,

discolored, and necrotic spots, as well as larger lesions due to herbivory (Fig. 4Ae-4Ah). In addition, there was more PM on their surfaces. The first results of the screening of BVOC emissions for the same species suggest significant differences in relative emissions between both sites (Fig. 4B).

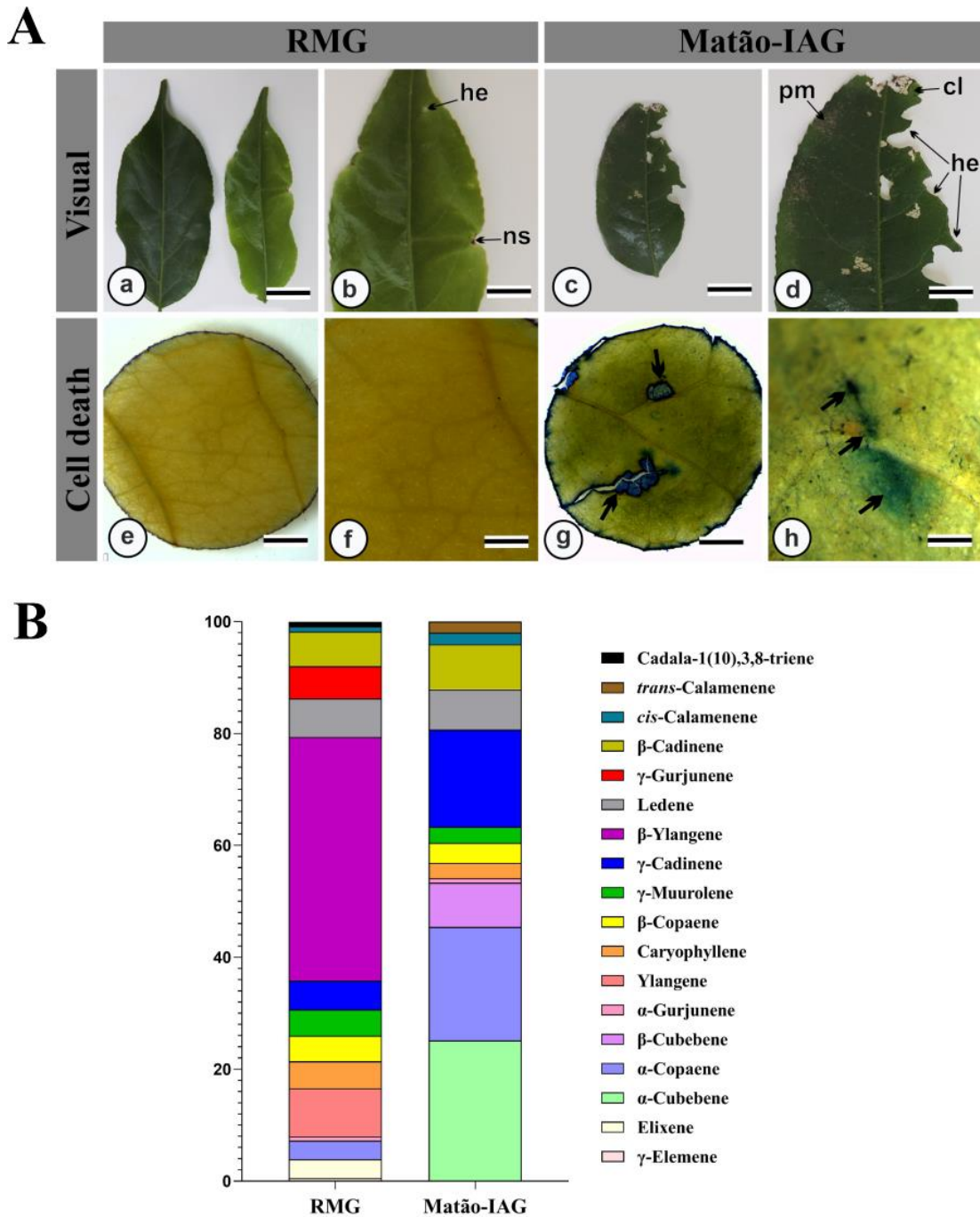


FIG. 4. (A) Anatomical parameters, including visual characterization (Aa-d) and evidence of cell death (Ae-h) of individuals at the RMG and Matão-IAG sites. Note the presence of necrotic spots

(ns), accumulation of particulate matter (pm), chlorosis (cl) and herbivory (he). Blue staining indicates a positive reaction for cell death (black arrows in Ah). Leaf photographs and staining with Evans' Blue dye were used to assess the extent of visual damage and cell necrosis. (B) Relative percentage of BVOCs emitted by *Casearia sylvestris* leaves during SOP2a (dry season). All BVOCs belong to the sesquiterpene class.

Meteorology during SOP3 (April 24 - June 29, 2023)

During SOP3, MASP was under the influence of anticyclonic circulation associated with the postfrontal high-pressure systems, moving northeast and merging with semi stationary South Atlantic Subtropical High, inducing surface winds from southeast. During this period, four cold fronts passed, characterized by sharp drops in temperature and increases in relative humidity (RH) (Fig. 5a and 5b), followed by changes in surface flow from weak southeast to strong prefrontal northwest winds (Fig. 5c and 5d). The heavy rain on May 31st, reaching 40mm in a single day, occurred during a cold front in RMG (Fig. 5b). The accumulated precipitation was 76 and 74 mm at both sites, indicating a homogeneous spatial pattern of precipitation in this MASP sector (Fig. SM1). On average, RMG temperatures and RH were $15 \pm 10^{\circ}\text{C}$ and $87 \pm 10\%$, respectively, and at Matão-IAG were $18 \pm 4^{\circ}\text{C}$ and $76 \pm 16\%$, respectively, being plausible to infer that these observed differences are caused by differences in altitude and land use (Table SM1). The wind patterns are remarkably consistent between both sites: predominantly below 5 m s^{-1} and from south and (Fig. 5c and 5d). Those values are within the climatological ones for the April-June period (Fig. SM2). As indicated in Figure 5, the diurnal evolution of meteorological variables at both sites are modulated by synoptic (cold-fronts), mesoscale systems such as sea-breeze (SB) and local-scale circulations induced by topography and land use and is also expected to influence the diurnal cycle of pollutant and non-pollutant concentrations in the atmosphere at MASP (Sánchez et al. 2025; Tito et al. 2024; Ferreira et al. 2024; Moreira et al. 2022a; Moreira et al. 2022b; Sánchez et al. 2022; Silveira et al. 2022; Oliveira et al. 2020; Sánchez et al. 2020; Ribeiro et al. 2018).

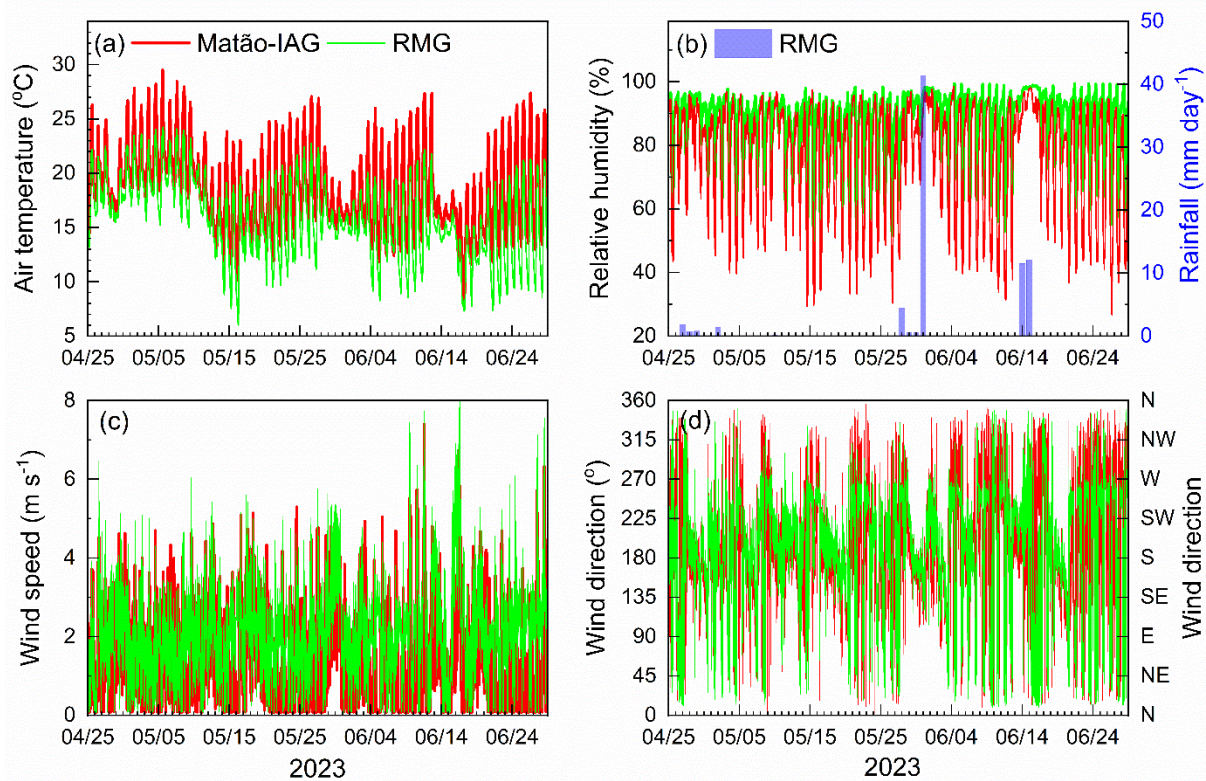


FIG. 5. Variability of 5-min average values of (a) temperature, (b) relative humidity, (c) wind speed, (d) wind directions at RMG (green) and Matão-IAG (red), from April 25 to June 29, 2023 (SOP3). Rainfall in (b) corresponds to the accumulated daily values at RMG.

Dynamical features and fluxes during SOP3

Low Level Jets (LLJ)

The main characteristics of low-level jet (LLJ) events at MASP were investigated in detail during the MCITY project (Sanchez et al. 2022). During SOP 3, the analysis of vertical wind speed profiles from rawinsondes carried out twice a day at Campo de Marte Airport (MARTE, Fig. SM1, Table SM1) indicated the presence of 52 LLJ events from April 1 to June 30 at MASP (62 % of the days). One event was identified on the night of April 23-24, reaching intensity of 11.8 m s^{-1} at 582 m (LLJ, Fig. 6a) and a no-LLJ event for May 8-9 (NO LLJ, Fig. 6b). The comparison indicates that CO_2 (Fig. 6c) and $\text{PM}_{2.5}$ (Fig. 6d) concentrations during the night with LLJ were systematically lower than those observed during the night without LLJ. This result corroborates previous findings by Sánchez et al. (2022), which indicate that the ventilation effect and horizontal advection associated with LLJ can reduce surface concentrations of aerosols and gases, such as $\text{PM}_{2.5}$ and CO_2 , during the night at MASP.

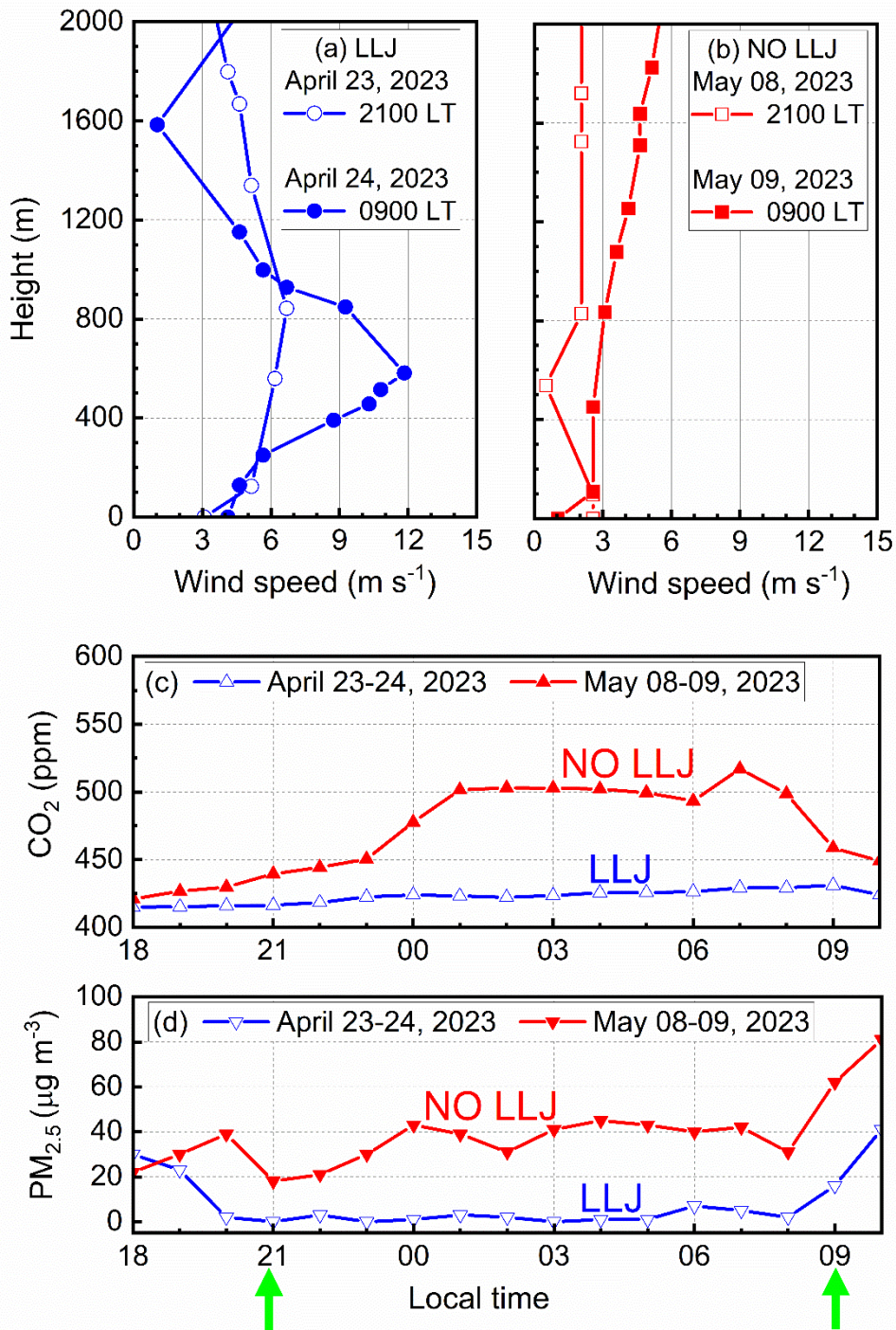


FIG. 6. Vertical wind speed profiles at 2100 and 0900 LT on (a) April 23-24, 2023, and (b) May 08-09, 2023, obtained from rawinsonde carried out in the Campo de Marte airport. The temporal evolution of days with LLJ (blue) and NO LLJ (red) events of (c) CO₂ concentration at Matão-IAG, and (d) PM_{2.5} in the CETESB air quality monitoring station located at the IPEN (CETESB – QUALAR, 2024). Green vertical arrows in (d) indicate rawinsonde released from local time.

Fluxes

The diel evolution of the main components of both the surface energy balance (SWB) and CO₂ fluxes are analyzed to identify the impact of land use in Matão-IAG and RMG, suburban ZCL 6 and rural ZCL A, respectively (Table SM1), on these properties. Those climate classifications relative to land use are described in the SM. The eddy covariance method which is detailed in the SM (Task 1 - *Procedure*) was applied to estimate vertical turbulent fluxes of sensible (H) and latent (LE) heat, and vertical turbulent flux of CO₂ (FCO₂), from turbulence measurements and using EddyPro algorithm (Fratine and Mauder, 2017) (Fig. 7). Footprint analyses are performed using the Flux Footprint Prediction (FFP) model developed by Kljun et al. (2015) and previously applied at MASP (Ferreira et al. 2024). The differences and commonalities in diel flux behavior between both sites generally depend on the presence of vegetation (evaporation, respiration, and photosynthesis). The FFP (Fig. SM6) shows that 90% of the turbulent fluxes, for Matão-IAG, follow the predominant wind direction between the south and southeast sectors, indicating the contribution of urban/suburban surfaces as the energy source area (Fig. SM6a and SM6b). Meanwhile, for RMG, the result shows the predominant south and southwest wind direction, indicating the rural/forest area as the main energy source area (Fig. SM6c and SM6d). On average, the SEB components in Matão-IAG and RMG reflect the predominantly suburban and rural land use of the sites (Fig. 7).

Net radiation at both sites shows similar amplitude while residue is systematically larger at Matão-IAG (Fig. 7a and 7b), indicating that there may be a larger store of energy in the suburban canopy at Matão-IAG (Ferreira et al. 2024). Although H and LE display a similar diurnal evolution at both sites, the large presence of vegetation in RMG is responsible for the larger values of LE. The presence of a dam southeast of the tower in RMG (Fig. 2d) may also contribute to the increase of LE.

Diurnal evolution of FCO₂ show an opposite trend during the day from 9 AM to 4 PM: negative values ($-15 \mu\text{mol m}^{-2} \text{s}^{-1}$) at RMG versus slightly positive ones ($+5 \mu\text{mol m}^{-2} \text{s}^{-1}$) at Matão-IAG, (Fig. 7b). At the forested RMG site, these above-canopy fluxes indicate the expected net uptake of CO₂ by photosynthesis which usually acts as a carbon sink. During the night, the RMG site shows positive CO₂ fluxes ($+5 \mu\text{mol m}^{-2} \text{s}^{-1}$) due to nighttime respiration. The pattern and intensity of CO₂ flux at the RMG are consistent with the one determined at other tropical forest sites like the Amazon (Carswell et al. 2002). The nighttime null fluxes at Matão-IAG rather indicate no net exchange of CO₂. The CO₂ flux patterns in urban areas are usually more heterogeneous being modulated by anthropogenic source emissions, vegetation

activity, urban underlying surface, and atmospheric stability (Cheng et al. 2017). Comparatively to European cities (Nicolini et al. 2022), the diurnal evolution of CO₂ flux at the Matão-IGAG (LCZ 6) display a similar behavior, with positive values during the entire day, but a smaller amplitude ($5 \mu\text{mol m}^{-2} \text{s}^{-1}$).

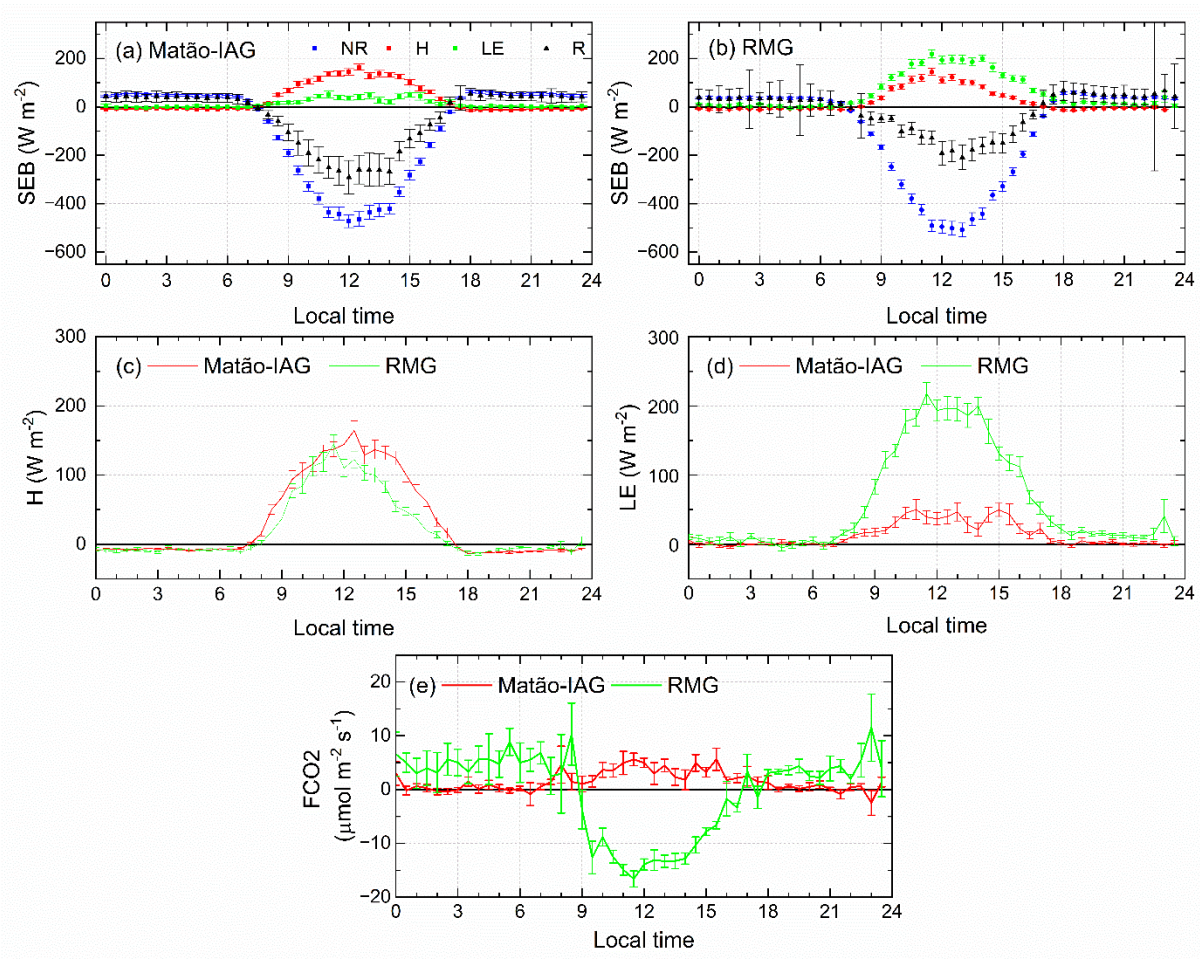


FIG. 7. Diel evolution of mean half-hourly values of surface energy balance (SEB) main components during SOP3 (April 21-May 24, 2023) at (a) Matão-IGAG, (b) RMG, corresponding to net radiation (NR), sensible (H) and latent (LE) heat fluxes, and residual ($R = NR+H+LE$). Comparison between Matão-IGAG and RMG for H, LE, and FCO₂ are indicated in (c), (d) and (e). Vertical bars correspond to standard error of the mean. Vertical fluxes are assumed to be positive when oriented upwards by convention.

Variability of gaseous precursors and secondary pollution during SOP3

The University of São Paulo campus, where the Matão-IAG site is located, is known to be an ozone hotspot within MASP (CETESB 2024). This has generally been attributed to emissions from surrounding heavy traffic and the emission of BVOCs by its urban forest, which favor local ozone production. The daily variability of ozone during the campaign period at Matão-IAG and RMG (SOP3a) reach comparable levels (45-50 ppb), with higher daily maxima in contrast to other regions within the MASP (35 ppb), despite a remarkably comparable temporal variability (Fig. 8). Such consistency indicates the regional signature of ozone production regardless of the location. The hourly cycle depicted in Figure 8b is typical of that of ozone in the MASP suggesting its photochemical production in the middle of the day. The nighttime behaviour of Matão-IAG closely follows that of the city, while RMG remains higher, likely less affected by nighttime NO emissions. From May 9th to May 14th during the cold front period, ozone levels are low (maxima of 30 ppb) and the diel cycle is no longer present.

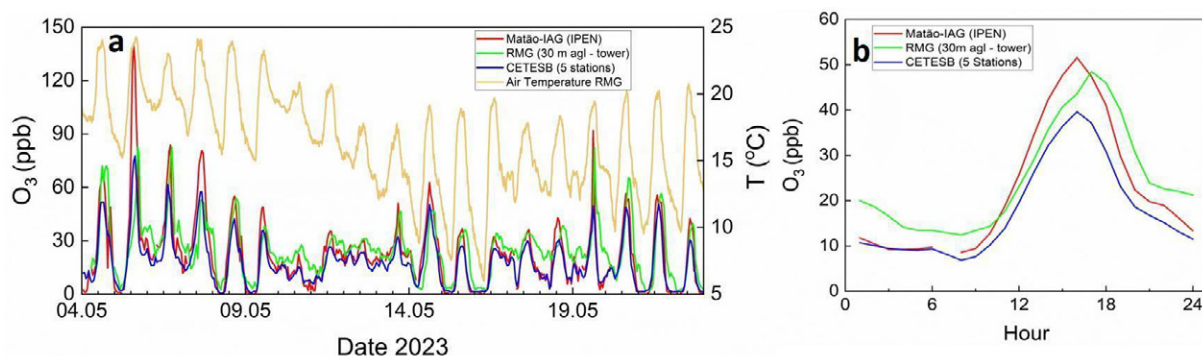


FIG. 8. Ozone mixing ratios during SOP3a at Matão-IAG (IPEN-USP), RMG (30m agl - tower) and an average of five CETESB stations across São Paulo city (Pinheiros, Grajaú, Ibirapuera, Interlagos, Carapicuíba). Panel (a) shows the time series and (b) the daily variability. Date in Local Time.

Figure 9 depicts the average concentrations of VOCs and the submicron chemical composition of PM at the RMG and Matão-IAG supersites. The VOC concentrations in Figure 9 are compared with literature values at MASP (CETESB 2024; Dominutti et al. 2016; Brito et al. 2015) and the Amazon (Yañez-Serrano et al. 2020). The compounds presented here are reactive species representative of biogenic (isoprene, sum of monoterpenes, speciated monoterpenes α - and β -pinenes, and their respective oxidation products) and anthropogenic (toluene and benzene) origins. Information is reported for species measured by PTR-ToF-MS

at the two supersites and by Gas Chromatography coupled to Flame Ionisation Detection (GC-FID) at the RMG supersite. The oxidation products of isoprene are the sum of Methyl Vinyl Ketone (MVK), Methacrolein (MACR) and Isoprene Hydroxy Hydroperoxide (ISOPOOH), while nopinone was selected as the monoterpene oxidation product (from β -pinene).

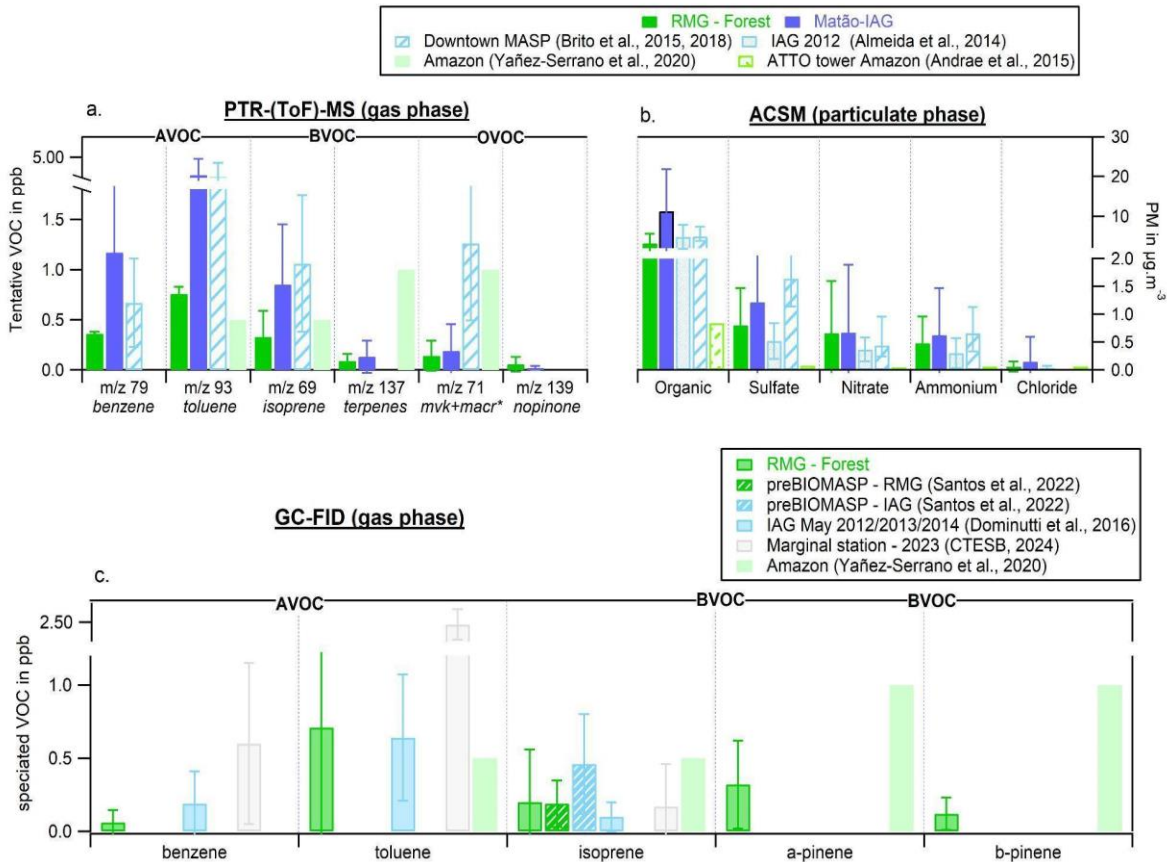


FIG. 9. Average mixing ratios ($\pm\sigma$) of VOCs (a and c) and average chemical composition ($\pm\sigma$) of non-refractory submicron aerosol (b) at RMG and Matão-IAG supersites during the BIOMASP+SOP3a. Those values are compared to other measurements in the MASP and the Amazon region. VOCs are reported for the PTR-ToF-Ms at the two sites and for the GC-FIDs at the RMG site. For (a), the horizontal axis represents the unit mass resolution for simplicity, and the corresponding tentative VOC, although the SOP3 data were calculated from high resolution observations. * mvk+macr stands for methacrolein + methyl vinyl ketone + isoprene hydroxy hydroperoxide.

For most of the gaseous and particulate species shown in Figure 9, the levels observed during BIOMASP+ SOP3a are consistent with those documented in previous field studies in the MASP, although they do not necessarily capture the same seasonal conditions or sampling site.

SOP3a took place in May 2023, during autumn, which marks the transition from the rainy to the dry season. In contrast, previous studies using PTR-MS and ACSM were conducted during different seasonal periods: Brito et al. (2018; 2015) reported observations from February 2013 (summer, rainy season) at a downtown site, and Almeida et al. (2014) from October 2012 (spring, transition from dry to rainy season) at the Matão-IAG site. Meanwhile, GC-FID observations (Santos et al. 2022; Dominutti et al. 2016) provided coverage over a full seasonal cycle for 2013-2015 and 2018-2019, respectively, and the data presented here were selected to coincide with SOP3.

Results show generally higher levels at Matão-IAG compared to RMG for the gaseous and particulate species regardless of their anthropogenic and biogenic origin. The scattering of the data is large, showing their high variability due to the contrasting environmental conditions encountered during SOP3a, as well as the reactivity of the gaseous species shown here. During SOP3a, primary BVOCs were about three times higher at Matão-IAG compared to RMG (0.85 and 0.33 ppb for isoprene, 0.24 and 0.08 ppb for monoterpenes), while aromatics were three to seven times higher (1.46 and 0.46 ppb for toluene, 0.83 and 0.13 ppb for benzene). These results are consistent with a pre-BIOMASP study reported by Santos et al. (2022), in which isoprene was observed to be approximately twice as high at the Matão-IAG site (0.46 ± 0.34 , 0.31 ± 0.1 (dry), 0.87 ± 0.3 (rainy)) compared to RMG (0.19 ± 0.16 , 0.11 ± 0.07 (dry), 0.37 ± 0.1 (rainy)), in 2018 and 2019. The authors assumed differences in vegetation types and the effect of Urban Heat Island. The additional fraction of anthropogenic isoprene and changes due to ozone exposure cannot be excluded.

Interestingly, observations of isoprene at Matão-IAG in May 2013 and 2015 depict significantly lower levels (0.10 ppb, Dominutti et al. 2016), suggesting a steady increase in isoprene over the past decade at this urban forested site captured by the same measurement technique (GC-FID). This increase is also evident when comparing the annual medians at IAG for 2013, 2014 and 2015, which are 0.16, 0.22 and 0.28 ppb, respectively (Dominutti et al. 2016). Taken together, the RMG and Matão-IAG sites show comparable isoprene levels but significantly lower monoterpene levels during SOP3 than those observed in the Central Amazon (Yañez-Serrano et al. 2020).

Isoprene oxidation products were observed at 0.27 and 0.14 ppb at Matão-IAG and RMG, respectively, while monoterpene oxidation products were at 0.04 and 0.01 ppb. The ratio of isoprene oxidation products to isoprene levels, which were used to assess OH exposure (e.g.

Santos et al. 2018), was 0.42 and 0.32 at RMG and Matão-IAG, respectively, suggesting comparable OH reactivity at both sites. This value is low compared to a ratio of 2 reported in the Central Amazon (Yañez-Serrano et al. 2020), indicating a strong dominance of local isoprene emissions at both RMG and Matão-IAG sites. This value is also in contrast to previous observations in the MASP, namely the downtown area, with a ratio closer to unity (Brito et al. 2015). This latter value was attributed to both transport from the Ibirapuera Park, a strong source of BVOCs within the MASP located a few kilometers from the downtown site, and primary anthropogenic emissions of MACR+MVK (Borbon et al. 2024).

The chemical composition of non-refractory submicron aerosol particles (i.e. NR-PM₁: Organic, Sulfate, Chloride, Ammonium and Nitrate) at both Matão-IAG and RMG sites are shown in Figure 10b. Results show an organic-dominated composition, with 82% and 61% of the mass on average at Matão-IAG and RMG, respectively, followed by Sulfate (8% and 16%) and Nitrate (4% and 13%). The strong dominance (over 80%) of Organics at Matão-IAG is confirmed by previous measurements conducted a decade earlier (Almeida et al. 2014), while observations at downtown MASP report a lower fraction (60%, Brito et al. 2018), even if the mass concentration remains equivalent. On average, NR-PM₁ concentrations during SOP3a were almost three times higher at Matão-IAG compared to RMG (13.9 and 5.1 $\mu\text{g m}^{-3}$, respectively), and roughly twice as high as those reported at the University site in October 2012 (6.0 $\mu\text{g m}^{-3}$, Almeida et al. 2014) and downtown in February-April 2013 (7.1 $\mu\text{g m}^{-3}$, Brito et al. 2018). Taken together, these results suggest the combined effect of anthropogenic and biogenic emissions at both sites, with the latter being dominated by isoprene.

Conclusion and way forward

The BIOMASP+ project is a Franco-Brazilian consortium with the objective of studying atmospheric biogenic-anthropogenic interactions and urban pollution in the context of the Brazilian Atlantic Forest in the Metropolitan Area of São Paulo. The two observation supersites are located in an Atlantic Forest Reserve outside the densely urbanized area (RMG) and in an urban forest inside the densely urbanized area (Matão-IAG). The towers were equipped with continuous instrumentation for the measurement of conventional meteorological parameters, energy, H₂O and CO₂ fluxes, and regulated pollutants during an extensive observation period. Special observation periods were dedicated to the quantification of BVOC emissions and to the characterization of the physical and chemical properties of gases and PM at the two contrasting supersites. The floristic survey showed the diversity of Atlantic Forest species at both locations,

with a greater presence of exotic species at Matão-IAG. Here, the preliminary results on BVOC emission composition, meteorology and dynamics and aerosol and gas composition during the first half of 2023 (SOP3 - fall, transition from the rainy to the dry season, April-June 2023) have been presented. The observations of SOPs of the year 2023 were consistent with the larger scale observations and have been placed in a historical perspective. First, results have shown higher levels of VOCs at Matão-IAG compared to RMG for the gaseous and particulate species regardless of their anthropogenic and biogenic origin. Moreover, the distribution of organic matter showed the combined effects of both anthropogenic and biogenic emissions at both sites, which seems to be enhanced at Matão-IAG. Second, the individual plant species from Matão-IAG usually presented more visual damages than the ones at RMG suggesting a stronger effect of urban stress. The composition of emitted BVOC changed at each location for a specific species. Finally, the coupling between emissions, air pollution and meteorology was demonstrated at both sites. The analysis of the detailed chemical composition of both gases and particles together with meteorological parameters will provide insights on their origin and on-going processes. Measurements of BVOC fluxes and launching of atmospheric profile soundings (temperature, relative humidity, pressure, and ozone) during SOP5 will complete the dataset in a 3D-dimension. At the end, all observations will constrain 0D and air quality modeling to understand the role of biogenic emissions in urban pollution (ozone and PM_{2.5}) and how this role is affected in a warming climate.

Acknowledgments

This study is funded by Fundação de Amparo à Pesquisa do Estado de São Paulo, Brazil (FAPESP-2020/07141-2) and Agence Nationale de la Recherche, France (ANR-20-784 CE01-0019). The Brazilian groups are supported by the Meteorology Post-Graduation Program of the University of São Paulo (IAG-USP) for the scholarships (CNPq and CAPES 001) and the special grants from CNPq (processes 312892/2023-3 and 402044/2022-3). The French groups are supported by the National Center for Scientific Research (CNRS/INSU - Terre et Univers), the PhD Joint Programme between CNRS and University of São Paulo and by the InVole Graduate Track from University Clermont Auvergne. IMT Nord Europe acknowledges financial support from the Labex CaPPA project, which is funded by the ANR through the PIA (Programme d'Investissement d'Avenir) under contract ANR-11-LABX-0005-01, the Regional Council "Hauts-de-France", and the European Regional Development Fund (ERDF). O. Murana was awarded an International Mobility Grant from the "Science for a Changing Planet" Graduate Programme, supported by the French government through the PIA (I-SITE ULNE / ANR-16-IDEX-0004 ULNE) managed by the ANR. Part of the measurements on the PM₁₀ yearly series are supported in France by the ANR ABS (ANR-21-CE01-0021-01). INERIS

acknowledges financial support from the French Ministry of Environment. The authors would like to especially thank the people involved in the preparation of the intensive field campaign and on the field: Evelyn Freney, Jean-Marc Pichon, Mickael Ribeiro, Laetitia Bouvier, Eduardo P. C. Gomes (*in memoriam*), Fernando Morais, Fabio Jorge, Alex Almeida dos Santos and Danilo de Andrade. Carine Gama provided the meteorological forecast during SOP3a. Thanks to SABESP for the logistical support for the installation and maintenance of the 30m tower at the Reserve of Morro Grande (Alto de Cotia Reservoir).

Data and availability statement

The metadata are available on the AERIS portal datacentre <https://www.aeris-data.fr/catalogue-biomasp>/<https://www.aeris-data.fr/projects/biomasp/>

References

- Almeida, G. P., Brito, J., Morales, C. A., Andrade, M. F., Artaxo, P. 2014: Measured and modelled cloud condensation nuclei (CCN) concentration in São Paulo, Brazil: The importance of aerosol size-resolved chemical composition on CCN concentration prediction. *Atmos. Chem. Phys.*, **14**, 7559–7572, <https://doi.org/10.5194/acp-14-7559-2014>.
- Alvares, C. A., Stape, J. L., Sentelhas, P. C., Gonçalves, J. L. M., Sparovek, G. 2013. Koppen’s climate classification map for Brazil, *Meteorol. Zeits.*, **22(6)**, 711–728, <https://doi.org/10.1127/0941-2948/2013/0507>.
- Araújo, H. H., and Coauthors, 2024: Atmospheric pollution affects the morphoanatomical and physiological responses of plants in urban Atlantic Forest remnants. *Environ. Sci. Pollut. Res.*, **32**, 4567–4587, <https://doi.org/10.1007/s11356-025-35952-0>.
- Arcosi, G.M, Miranda, F.D.A, Martello, M., Smaniatto, D.A, Sartor, L.R. 2019: Estimating Biomass of Black Oat Using UAV-Based RGB Imaging. *Agronomy*, **9**, 344, <https://doi.org/10.3390/agronomy9070344>.
- Baray, J.-L., and Coauthors, 2020: Cézeaux-Aulnat-Opme-Puy De Dôme: a multi-site for the long-term survey of the tropospheric composition and climate change. *Atmos. Meas. Tech.*, **13**, 3413–3445, <https://doi.org/10.5194/amt-13-3413-2020>.
- Borbon, A., Salameh, T., Sauvage, S., Afif, C. 2024: Light oxygenated volatile organic compound concentrations in an Eastern Mediterranean urban atmosphere rivalling those in megacities. *Environ. Pollut.*, **350**, 123797, <https://doi.org/10.1016/j.envpol.2024.123797>.

- Brito, J., Wurm, F., Yáñez-Serrano, AM., Vicente de Assunção, J., Godoy, M., Artaxo, P. 2015: Vehicular Emission Ratios of VOCs in a Megacity Impacted by Extensive Ethanol Use: Results of Ambient Measurements in São, Paulo, Brazil, *Environ. Sci. Technol.*, **49(19)**, 11381–11387, <http://dx.doi.org/10.1021/acs.est.5b03281>.
- Brito, J., Carbone, S., Santos, D. A. M., Dominutti, P., Alves, N. O., Rizzo, L. V., Artaxo, A. 2018: Disentangling vehicular emission impact on urban air pollution using ethanol as a tracer. *Sci. Rep.* **8**, 10679, <https://doi.org/10.1038/s41598-018-29138-7>.
- Calfapietra, C., Fares, S., Manes, F., Morani, A., Sgrigna, G., Loreto, F. 2013: Role of Biogenic Volatile Organic Compounds (BVOC) emitted by urban trees on ozone concentration in cities: a review. *Environ Pollut.*, **183**, 71-80, <https://doi.org/10.1016/j.envpol.2013.03.012>.
- Carlton, A. G., Wiedinmyer, C., Kroll, J. H. 2009: A review of Secondary Organic Aerosol (SOA) formation from isoprene. *Atmos. Chem. Phys.*, **9**, 4987–5005, <https://doi.org/10.5194/acp-9-4987-2009>.
- CETESB (1994), Relatório de qualidade do ar no estado de São Paulo 1993, 85 p. (Série Relatórios / CETESB, ISSN 0103-4103), <https://cetesb.sp.gov.br/ar/publicacoes-relatorios/>.
- CETESB (2024), Qualidade do ar no Estado de São Paulo 2023, 162 p. (Série Relatórios / CETESB, ISSN 0103-4103), <https://cetesb.sp.gov.br/ar/publicacoes-relatorios/>.
- CETESB-QUALAR, 2024 - <https://cetesb.sp.gov.br/ar/qualar/>
- Chameides, W. L., Lindsay, R. W., Richardson, J., Kiang, C. S. 1988: The role of biogenic hydrocarbons in urban photochemical smog: Atlanta as a case study. *Science*, **241**,1473-1475, <https://doi.org/10.1126/science.3420404>.
- Chin, M., and Coauthors. 2002: Tropospheric aerosol optical thickness from the GOCART model and comparisons with satellite and sun photometer measurements. *J. Atmos. Sci.*, **59**, 461-483, [https://doi.org/10.1175/1520-0469\(2002\)059<0461:TAOTFT>2.0.CO;2](https://doi.org/10.1175/1520-0469(2002)059<0461:TAOTFT>2.0.CO;2).
- Churkina, G., Kuik, F., Bonn, B., Lauer, A., Grote, R., Tomiak, K., Butler, T. M. 2017: Effect of VOC Emissions from Vegetation on Air Quality in Berlin during a Heatwave. *Environ. Sci. Technol.*, **51**, 6120–6130, <https://doi.org/10.1021/acs.est.6b06514>.
- Crippa, M., Oreggioni, G., Guizzardi, D., Muntean, M., Schaaf, E., Lo Vullo, E., Solazzo, E., Monforti-Ferrario, F., Olivier, J., Vignati, E. 2019: Fossil CO₂ and GHG emissions of all world countries – 2019 Report, EUR 29849 EN, Publications Office of the European Union, Luxembourg, JRC117610, https://doi.org/10.2760/https://docs.google.com/document/d/1tXPWfR5MIzNf8mqzgSd1RAyOhIIM4irx/edit?usp=drive_link&oid=110527194285461024562&rtpof=true&sd=true687800.

- Crippa, M., Solazzo, E., Huang, G. et al. 2020: High resolution temporal profiles in the Emissions Database for Global Atmospheric Research. *Sci. Data*, **7**, 121, <https://doi.org/10.1038/s41597-020-0462-2>.
- Emmons, L.K., and Coauthors, 2010: Description and evaluation of the Model for Ozone and Related Chemical Tracers, version 4 (MOZART-4). *Geosci. Model Dev.*, **3**, 43-67, <https://doi.org/10.5194/gmd-3-43-2010>.
- Déméautis, T., Delles, M., Tomaz, S., Monneret, G., Glehen, O., Devouassoux, G., George, C., Bentaher, A. 2022: Pathogenic Mechanisms of Secondary Organic Aerosols. *Chem. Res. Toxicol.*, **35**, 1146–1161, <https://doi.org/10.1021/acs.chemrestox.1c00353>.
- Dominutti, P. A., Nogueira, T., Borbon, A., Andrade, M. F., Fornaro, A. 2016: One-year of NMHCs hourly observations in São Paulo megacity: meteorological and traffic emissions effects in a large ethanol burning context. *Atmos. Environ.*, **142**, 371–382. <https://doi.org/10.1016/j.atmosenv.2016.08.008>.
- Dominutti, P.A., Thera, B., Colomb, A., Borbon, A. 2024: Composition and chemical processing of volatile organic compounds in boundary layer polluted plumes: Insights from an airborne Q-PTR-MS on-board the French ATR-42 aircraft, *Sci. Total Environ.*, **941**, <https://doi.org/10.1016/j.scitotenv.2024.173311>.
- Donahue, N. M., Robinson, A.L., Stanier, C. O., Pandis, S.N. 2006: Coupled partitioning, dilution, and chemical aging of semivolatile organics. *Environ. Sci. Technol.*, **40(8)**, 2635-2643. <https://doi.org/10.1021/es052297c>.
- Farhat, M., Pailler, L., Camredon, M., Maison, A., Sartelet, K., Patryl, L., Armand, P., Afif, C., Borbon A., Deguillaume L. 2025: Investigating the role of anthropogenic terpenoids in urban secondary pollution under summer conditions by a box modeling approach. *Environ. Sci.: Atmos.*, **5**, 574-590, <https://doi.org/10.1039/d4ea00112e>.
- Ferreira, M. J., Oliveira, A. P., Silveira, L. C., Codato, G., Fornaro, A., Borbon, A. 2024: Surface energy balance in a suburban area of the megacity of São Paulo - Seasonal variation and closure. *Urban Clim.*, **56**, 102008, <https://doi.org/10.1016/j.uclim.2024.102008>.
- Fierravanti, A., Fierravanti, E., Coccozza, C., Tognetti, R., Rossi, S. 2017: Eligible reference cities in relation to BVOC-derived O₃ pollution. *Urban For. Urban Green.*, **28**, 73-80, <https://doi.org/10.1016/j.ufug.2017.09.012>.
- Fitzky, A. C., Sandén, H., Karl, T., Fares, S., Calfapietra, C., Grote, R., Saunier, A., Rewald, B. 2019: The Interplay Between Ozone and Urban Vegetation — BVOC Emissions, Ozone Deposition, and Tree Ecophysiology. *Front. For. Glob. Change*, **2**, 50, <https://doi.org/10.3389/ffgc.2019.00050>.

- Fornaro, A., Gutz, I. G. R. 2006: Wet deposition and related atmospheric chemistry in the São Paulo metropolis, Brazil. Part 3: Trends in precipitation chemistry during 1983–2003. *Atmos. Environ.*, **40**, 5893–5901, <https://doi.org/10.1016/j.atmosenv.2005.12.007>.
- Fratini, G., Mauder, M. 2014: Towards a consistent eddy-covariance processing: an intercomparison of EddyPro and TK3. *Atmos. Meas. Tech.*, **7(7)**, 2273–2281, <https://doi.org/10.5194/amt-7-2273-2014>.
- Freitas, A. D., Fornaro, A. 2022: Atmospheric Formaldehyde Monitored by TROPOMI Satellite Instrument throughout 2020 over São Paulo State, Brazil. *Remote Sens.*, **14(13)**, 3032, <https://doi.org/10.3390/rs14133032>.
- Frutuoso, F. S., Alves, C. M.A.C., Araújo, S. L., Serra, D. S., Barros, A. L. B. P., Cavalcante, F. S. A., Araújo, R. S., Policarpo, N. A., Oliveira, M. L. M. 2023: Assessing light flex-fuel vehicle emissions with ethanol/gasoline blends along an urban corridor: A case of Fortaleza/Brazil. *Int. J. Transp. Sci. Technol.*, **12(2)**, 447–459, <https://doi.org/10.1016/j.ijst.2022.04.001>.
- Fundação SOS Mata Atlântica; INPE. Atlas dos remanescentes florestais da Mata Atlântica: período de 2021/2022, Relatório Técnico. São Paulo: Fundação SOS Mata Atlântica, 2023. 61p. https://cms.sosma.org.br/wp-content/uploads/2023/05/SOSMAAtlas-da-Mata-Atlantica_2021-2022-1.pdf
- Gao, Y., Ma, M., Yan, F., Su, H., Wang, S., Liao, H., Zhao, B., Wang, X., Sun, Y., Hopkins, J. R., Chen, Q., Fu, P., Lewis, A. C., Qiu, Q., Yao, X., Gao, H. 2022: Impacts of biogenic emissions from urban landscapes on summer ozone and secondary organic aerosol formation in megacities, *Sci. Total Environ.*, **814**, 152654, <https://doi.org/10.1016/j.scitotenv.2021.152654>.
- Gao, Z., Zhou, X., 2024: A review of the CAMx, CMAQ, WRF-Chem and NAQPMS models: Application, evaluation and uncertainty factors, *Environ. Pollut.*, **343**, 123183, <https://doi.org/10.1016/j.envpol.2023.123183>.
- Glojek, K., and Coauthors, 2024: Annual variation of source contributions to PM₁₀ and oxidative potential in a mountainous area with traffic, biomass burning, cement-plant and biogenic influences. *Environ. Intern.*, **189**, 108787, <https://doi.org/10.1016/j.envint.2024.108787>.
- Gkatzelis, G. I., and Coauthors, 2018: Gas-to-particle partitioning of major biogenic oxidation products: a study on freshly formed and aged biogenic SOA. *Atmos. Chem. Phys.*, **18(17)**, 12969–12989, <https://doi.org/10.5194/acp-18-12969-2018>.
- Grell, G. A., Peckham, S. E., Schmitz, R., McKeen, S. A., Frost, G., Skamarock, W. C., Eder, B. 2005: Fully coupled “online” chemistry within the WRF model. *Atmos. Environ.*, **39**, 6957–6975, <https://doi.org/10.1016/j.atmosenv.2005.04.027>.

- Gu, S., Guenther, A., Faiola, C. 2021: Effects of Anthropogenic and Biogenic Volatile Organic Compounds on Los Angeles Air Quality. *Environ. Sci. Technol.*, **55(18)**, 12191-12201, <https://doi.org/10.1021/acs.est.1c01481>.
- Guenther, A., Karl, T., Harley, P., Wiedinmyer, C., Palmer, P. I., and Geron, C. 2006: Estimates of global terrestrial isoprene emissions using MEGAN (Model of Emissions of Gases and Aerosols from Nature). *Atmos. Chem. Phys.*, **6**, 3181–3210, <https://doi.org/10.5194/acp-6-3181-2006>.
- Hallquist, M., and Coauthors, 2009: The formation, properties and impact of secondary organic aerosol: current and emerging issues. *Atmos. Chem. Phys.*, **9**, 5155–5236, <https://doi.org/10.5194/acp-9-5155-2009>.
- Heald, C. L., Kroll, J. H. 2020: The fuel of atmospheric chemistry: Toward a complete description of reactive organic carbon. *Sci. Adv.*, **6**, eaay8967, <https://doi.org/10.1126/sciadv.aay8967>.
- Kang, E., Root, M. J., Toohey, D. W., Brune, W. H. 2007: Introducing the concept of Potential Aerosol Mass (PAM), *Atmos. Chem. Phys.*, **7**, 5727–5744, <https://doi.org/10.5194/acp-7-5727-2007>.
- Kljun, N., Calanca, P., Rotach, M. W., Schmid, H. P. 2015: A simple two-dimensional parameterization for Flux Footprint Prediction (FFP). *Geosci. Model Dev.*, **8**, 3695–3713, <https://doi.org/10.5194/gmd-8-3695-2015>.
- Kroll, J. H., Ng, N. L., Murphy, S. M., Flagan, R. C., Seinfeld, J. H. 2006: Secondary Organic Aerosol Formation from Isoprene Photooxidation, *Environ. Sci. Technol.*, **40(6)**, 1869-1877, <https://doi.org/10.1021/es0524301>.
- Lambe, A. T., Ahern, A. T., Williams, L. R., Slowik, J. G., Wong, J. P. S., Abbatt, J. P. D., Brune, W. H., Ng, N. L., Wright, J. P., Croasdale, D. R., Worsnop, D. R., Davidovits, P., Onasch, T. B. 2011: Characterization of aerosol photooxidation flow reactors: heterogeneous oxidation, secondary organic aerosol formation and cloud condensation nuclei activity measurements. *Atmos. Measure. Techn.*, **4**, 445–461, <https://doi.org/10.5194/amt-4-445-2011>.
- Li, R., Palm, B. B., Ortega, A. M., Hlywiak, J., Hu, W., Peng, Z., Day, D. A., Knote, C., Brune, W. H., de Gouw, J. A., Jimenez, J. L. 2015: Modeling the Radical Chemistry in an Oxidation Flow Reactor: Radical Formation and Recycling, Sensitivities, and the OH Exposure Estimation Equation. *J. Phys. Chem. A*, **119**, 4418–4432, <https://doi.org/10.1021/jp509534k>.
- Li, K., Zhang, X., Zhao, B., Bloss, W. J., Lin, C., White, S., Yu, H., Chen, L., Geng, C., Yang, W., Azzi, M., George, C., Bai, Z. 2022: Suppression of anthropogenic secondary organic aerosol formation by isoprene, *npj. Clim. Atmos. Sci.*, **5**, 1–9, <https://doi.org/10.1038/s41612-022-00233-x>.
- Liaskoni, M., Huszár, P., Bartík, L., Prieto Perez, A. P., Karlický, J., Šindelářová, K. 2024: The long-term impact of biogenic volatile organic compound emissions on urban ozone patterns over central

- Europe: contributions from urban and rural vegetation, *Atmos. Chem. Phys.*, **24**, 13541–13569, <https://doi.org/10.5194/acp-24-13541-2024>.
- Lima, R.A.F., Oliveira, A.A., Pitta, G.R., Gasper, A. L., Vibrans, A. C., Chave, J., ter Steege, H., Prado, P. I. 2020: The erosion of biodiversity and biomass in the Atlantic Forest biodiversity hotspot. *Nat Commun.*, **11**, 6347, <https://doi.org/10.1038/s41467-020-20217-w>.
- Mardoñez, V., and Coauthors, 2023: Source apportionment study on particulate air pollution in two high-altitude Bolivian cities: La Paz and El Alto. *Atmos. Chem. Phys.*, **23**, 10325–10347, <https://doi.org/10.5194/acp-23-10325-2023>.
- Marengo, J. A., Souza, C. M. Jr, Thonicke, K., Burton, C., Halladay, K., Betts, R. A., Alves, L. M., Soares, W. R. 2018: Changes in Climate and Land Use Over the Amazon Region: Current and Future Variability and Trends. *Front. Earth Sci.*, **6**, 228, <https://doi.org/10.3389/feart.2018.00228>.
- McFiggans, G., and Coauthors, 2019: Secondary organic aerosol reduced by mixture of atmospheric vapours. *Nature*, **565**, 587–593, <https://doi.org/10.1038/s41586-018-0871-y>.
- MMA, 2022. Ministério do Meio Ambiente, Portaria MMA Nº 148, 7 de junho de 2022. https://www.icmbio.gov.br/cepsul/images/stories/legislacao/Portaria/2020/P_mma_148_2022_altera_anexos_P_mma_443_444_445_2014_atualiza_especies_amecadas_extincao.pdf
- Moreira, G.A., Oliveira, A. P., Sánchez, M. P., Codato, G., Lopes, F. J. S., Landulfo, E., Marques Filho, E. P. 2022a: Performance assessment of aerosol-lidar remote sensing skills to retrieve the time evolution of the urban boundary layer height in the Metropolitan Region of São Paulo City, Brazil. *Atmos. Res.*, **277**, 106290, <https://doi.org/10.1016/j.atmosres.2022.106290>.
- Moreira, G.A., Oliveira, A. P., Codato, G., Sánchez, M P., Tito, J. V., Hussni e Silva, L. A., Silveira, L. C., Silva, J. J., Lopes, F. J. S., Landulfo, E. 2022b: Assessing Spatial Variation of PBL Height and Aerosol Layer Aloft in São Paulo Megacity Using Simultaneously Two Lidar during Winter 2019. *Atmos.*, **13**, 611, <https://doi.org/10.3390/atmos13040611>.
- Moreno, C. I., and Coauthors, 2024: Tropical tropospheric aerosol sources and chemical composition observed at high altitude in the Bolivian Andes. *Atmos. Chem. Phys.*, **24**, 2837–2860, <https://doi.org/10.5194/acp-24-2837-2024>.
- Moura, B. B., Bolsoni, V. P., de Paula M. D., Dias G. M., Souza, S. R. 2022: Ozone Impact on Emission of Biogenic Volatile Organic Compounds in Three Tropical Tree Species From the Atlantic Forest Remnants in Southeast Brazil. *Front. Plant Sci.*, **13**, 879039, <https://doi.org/10.3389/fpls.2022.879039>.
- Ng, N. L., Kroll, J. H., Chan, A. W. H., Chhabra, P. S., Flagan, R. C., Seinfeld, J. H. 2007: Secondary organic aerosol formation from m-xylene, toluene, and benzene. *Atmos. Chem. Phys.*, **7**, 3909–3922, <https://doi.org/10.5194/acp-7-3909-2007>.

- Nicolini, G., and Coauthors, 2022: Direct observations of CO₂ emission reductions due to COVID-19 lockdown across European urban districts. *Sci. Total Environ.*, **830**, 154662, <https://doi.org/10.1016/j.scitotenv.2022.154662>.
- Oliveira, A.P., and Coauthors, 2020: Assessing urban effects on the climate of metropolitan regions of Brazil - Preliminary results of the MCITY BRAZIL project. *Explor. Environ.Sci. Res.*, **1(1)**, 38–77, <https://dx.doi.org/10.47204/EESR.1.1.2020.038-077>.
- Orlando, J.P., Alvim, D.S., Yamazaki, A., Corrêa, S.M., Gatti, L.V. 2010: Ozone precursors for the São Paulo Metropolitan Area. *Sci. Total Environ.*, **408(7)**, 1612-1620, <https://dx.doi.org/10.1016/j.scitotenv.2009.11.060>.
- Peng, Z. Jimenez, J. L. 2020: Radical chemistry in oxidation flow reactors for atmospheric chemistry research. *Chem. Soc. Rev.*, **49**, 2570-2616, <https://doi.org/10.1039/C9CS00766K>.
- Penuelas, J., Staudt, M. 2010: BVOCs and global change. *Trends in Plant Sci.*, **15(3)**, 133-144, <https://doi.org/10.1016/j.tplants.2009.12.005>.
- Peron, A., Graus, M., Striednig, M., Lamprecht, C., Wohlfahrt, G., and Karl, T. 2024: Deciphering anthropogenic and biogenic contributions to selected non-methane volatile organic compound emissions in an urban area. *Atmos. Chem. Phys.*, **24**, 7063–7083, <https://doi.org/10.5194/acp-24-7063-2024>.
- Petäjä, T., and Coauthors, 2021: Added Value of Vaisala AQT530 Sensors as a Part of a Sensor Network for Comprehensive Air Quality Monitoring. *Front. Environ. Sci.*, **9**, 719567, <https://doi.org/10.3389/fenvs.2021.719567>.
- Ren, Y., Qu, Z., Du, Y., Xu, R., Ma, D., Yang, G., Shi, Y., Fan, X., Tani, A., Guo, P., Ge, Y., Chang, J. 2017: Air quality and health effects of biogenic volatile organic compounds emissions from urban green spaces and the mitigation strategies. *Environ. Pollut.*, **230**, 849-861, <https://doi.org/10.1016/j.envpol.2017.06.049>.
- Ribeiro, F.N.D., Oliveira, A.P., Soares, J., Miranda, R.M., Barlage, M., Chen, F. 2018: Effect of sea breeze propagation on the urban boundary layer of the metropolitan region of Sao Paulo, Brazil. *Atmos. Res.*, **214**, 174-188, <https://doi.org/10.1016/j.atmosres.2018.07.015>.
- Rocco, M., and Coauthors, 2024: VELVET: an enclosure vegetation system to measure BVOC emission fingerprints in temperate and tropical climates. *Front. Environ. Sci.*, **12**, 1372931, <https://doi.org/10.3389/fenvs.2024.1372931>.
- Romero-Puertas, M. C., Rodríguez-Serrano, M., Corpas, F. J., Gómez, M., Del Río, L. A., Sandalio, L. M. 2004: Cadmium induced subcellular accumulation of O₂- and H₂O₂ in pea leaves. *Plant, Cell Environ.*, **27**, 1122-1134, <https://doi.org/10.1111/j.1365-3040.2004.01217.x>.

- Rosa, M. R., Brancalion, P. H. S., Crouzeilles, R., Tambosi, L. R., Piffer, P. R., Lenti, F. E. B., Hirota, M., Santiami, E., Metzger, J. P. 2021: Hidden destruction of older forests threatens Brazil's Atlantic Forest and challenges restoration programs. *Sci. Adv.*, **7**, eabc4547, <https://doi.org/10.1126/sciadv.abc454>.
- Samaké, A., and Coauthors, 2019: Polyols and glucose as tracers of primary biogenic organic aerosol: influence of environmental factors on ambient air concentrations and spatial distribution over France. *Atmos. Chem. Phys.*, **19**, 3357–3374, <https://doi.org/10.5194/acp-19-3357-2019>, 2019.
- Samaké, A., Bonin, A., Jaffrezo, J.L., Taberlet, P., Uzu, G., Conil S., Favez, O., Thomasson, A, Chazeau, B., Marchand, N., Martins, J. M. F. 2021: Variability of the microbiome in atmospheric PM₁₀ in several climatic regions of France. *Front. Microbiol.*, **11**, 576750, <https://doi.org/10.3389/fmicb.2020.576750>.
- Sánchez, M.P., Oliveira, A.P., Varona, R.P., Tito, J.V., Codato, G., Ribeiro, F.N.D., Marques Filho, E.P., Silveira, L.C. 2020: Rawinsonde-based analysis of the urban boundary layer in the metropolitan region of São Paulo, Brazil. *Earth and Space Sci.*, **7**, e2019EA000781, <https://doi.org/10.1029/2019EA000781>.
- Sánchez, M.P., Oliveira, A.P., Varona, R.P., Tito, J.V., Codato, G., Ynoue, R.Y., Ribeiro, F.N.D., Marques Filho, E.P., Silveira, L.C. 2022: Observational investigation of the low-level jets in the metropolitan region of São Paulo, Brazil. *Earth and Space Sci.*, **9(9)**, e2021EA002190, <https://doi.org/10.1029/2021EA002190>.
- Salvo, A., Geiger, F.M. 2014: Reduction in local ozone levels in urban São Paulo due to a shift from ethanol to gasoline use. *Nature Geoscience*, **7**, 450–458, <https://doi.org/10.1038/ngeo2144>.
- Santos, F., Longo, K., Guenther, A., Kim, S., Gu, D., Oram, D., Forster, G., Lee, J., Hopkins, J., Brito, J., Freitas, S. 2018: Biomass burning emission disturbances of isoprene oxidation in a tropical forest. *Atmos. Chem. Phys.*, **18**, 12715–12734, <https://doi.org/10.5194/acp-18-12715-2018>.
- Santos, T. C. Dominutti, P., Pedrosa, G. S., Coelho, M. S., Nogueira, T., Borbon, A., Souza, S. R., Fornaro, A. 2022: Isoprene in urban Atlantic forests: Variability, origin, and implications on the air quality of a subtropical megacity, *Sci. Total Environ.*, **824**, 153728, <https://doi.org/10.1016/j.scitotenv.2022.153728>.
- Shilling, J. E., and Coauthors, 2013: Enhanced SOA formation from mixed anthropogenic and biogenic emissions during the CARES campaign. *Atmos. Chem. Phys.*, **13**, 2091–2113, <https://doi.org/10.5194/acp-13-2091-2013>.
- Schuch, D., Freitas, E. D., Ibarra, S. E., Martins, L. D., Carvalho, V. S. B., Ramin, B. F., Silva, J. S., Martins, J. A., Andrade, M. F. 2019: A two decades study on ozone variability and trend over the

main urban areas of the São Paulo state, Brazil. *Environ. Sci. Pollut. Res.*, **26**, 31699–31716, <https://doi-org.insu.bib.cnrs.fr/10.1007/s11356-019-06200-z>.

Silveira, L. C., Oliveira, A. P., Codato, G., Sanchez, M. P., Fornaro, A. 2024: Spectral Properties of Turbulence in a Suburban Area of São Paulo Megacity. *Boundary-Layer Meteor.*, **190**, 44, <https://doi.org/10.1007/s10546-024-00877-7>.

Silveira, L. C., Oliveira, A.P., Sánchez, M.P., Codato, G., Ferreira, M.J., Marques Filho, E.P., Božnar, M. Z., Mlakar, P. 2022: Observational Investigation of the Statistical Properties of Surface-Layer Turbulence in a Suburban Area of São Paulo, Brazil: Objective Analysis of Scaling-Parameter Accuracy and Uncertainties. *Boundary-Layer Meteor.* **185**, 161-195, <https://doi.org/10.1007/s10546-022-00726-5>.

Sindelarova, K., Granier, C., Bouarar, I., Guenther, A., Tilmes, S., Stavrou, T., Müller, J.-F., Kuhn, U., Stefani, P., Knorr, W. 2014: Global data set of biogenic VOC emissions calculated by the MEGAN model over the last 30 years. *Atmos. Chem. Phys.*, **14**, 9317–9341, <https://doi.org/10.5194/acp-14-9317-2014>.

Srivastava, D., Vu, T.V., Tong, S., Shi, Z., Harrison, R. M. 2022: Formation of secondary organic aerosols from anthropogenic precursors in laboratory studies. *npj Clim. Atmos. Sci.* **5**, 22, <https://doi.org/10.1038/s41612-022-00238-6>.

Srivastava, M., and Coauthors, 2017: Recent advances in understanding secondary organic aerosol: Implications for global climate forcing. *Rev. Geophys.*, **55**, 509–559, <https://doi.org/10.1002/2016RG000540>.

Stevens, C. J., Bell, J. N. B., Brimblecombe, P., Clark, C. M., Dise, N. B., Fowler, D., Lovett, G. M., Wolsey, P.A. 2020: The impact of air pollution on terrestrial managed and natural vegetation. *Phil. Trans. R. Soc. A*, **378**, 20190317, <http://dx.doi.org/10.1098/rsta.2019.0317>.

Takeuchi, M., Berkemeier, T., Eris, G., Ng, N. L. 2022: Non-linear effects of secondary organic aerosol formation and properties in multi-precursor systems, *Nat. Commun.*, **13**, 7883, <https://doi.org/10.1038/s41467-022-35546-1>.

Tsigaridis, K., Kanakidou, M. 2018: The present and future of Secondary Organic Aerosol direct forcing on climate. *Curr. Clim. Change Rep.*, **4**, 84–98, <https://doi.org/10.1007/s40641-018-0092-3>.

Torres, F. D. R., Oliveira, A. P., Silveira L. C. 2023: Sensible, latent heat and store energy fluxes in the suburban São Paulo Megacity: seasonal and interannual variations and empirical modeling. *Inter. J. Hydro.*, **7(4)**, 151–158, <https://doi.org/10.15406/ijh.2023.07.00351>.

Yañez-Serrano, A. M., and Coauthors, 2020: Amazonian biogenic volatile organic compounds under global change, *Glob. Chang. Biol.*, **26(9)**, 4722–4751, <https://doi.org/10.1111/gcb.15185>.

- Vara-Vela, A.L., Andrade, M.F., Kumar, P., Ynoue, R.Y., Muñoz, A.G. 2016: Impact of vehicular emissions on the formation of fine particles in the Sao Paulo Metropolitan Area: a numerical study with the WRF-Chem model. *Atmos. Chem. Phys.*, **16**, 777–797, <https://doi.org/10.5194/acp-16-777-2016>.
- Voliotis, A., Du, M., Wang, Y., Shao, Y., Alfarra, M. R., Bannan, T. J., Hu, D., Pereira, K. L., Hamilton, J. F., Hallquist, M., Mentel, T. F., McFiggans, G. 2022a: Chamber investigation of the formation and transformation of secondary organic aerosol in mixtures of biogenic and anthropogenic volatile organic compounds. *Atmos. Chem. Phys.*, **22**, 14147–14175, <https://doi.org/10.5194/acp-22-14147-2022>.
- Voliotis, A., Du, M., Wang, Y., Shao, Y., Bannan, T. J., Flynn, M., Pandis, S. N., Percival, C. J., Alfarra, M. R., McFiggans, G. 2022b: The influence of the addition of isoprene on the volatility of particles formed from the photo-oxidation of anthropogenic–biogenic mixtures, *Atmos. Chem. Phys.*, **22**, 13677–13693, <https://doi.org/10.5194/acp-22-13677-2022>.
- von der Weiden, S.-L., Drewnick, F., Borrmann, S. 2009: Particle Loss Calculator – a new software tool for the assessment of the performance of aerosol inlet systems. *Atmos. Meas. Tech.*, **2**, 479–494, <https://doi.org/10.5194/amt-2-479-2009>.
- Wennberg, P. O., Bates, K. H., Crouse, J. D., Dodson, L. G., McVay, R. C., Mertens, L. A., Nguyen, T. B., Praske E., Schwantes, R. H., Smarte, M. D., St Clair, J. M., Teng, A. P., Zhang, X., Seinfeld, J. H. 2018: Gas-Phase Reactions of Isoprene and Its Major Oxidation Products. *Chem. Rev.*, **118**(7), 3337–3390, <https://doi.org/10.1021/acs.chemrev.7b00439>.
- WHO global air quality guidelines. Particulate matter (PM_{2.5} and PM₁₀), ozone, nitrogen dioxide, sulfur dioxide and carbon monoxide. Geneva: World Health Organization; 2021. ISBN 978-92-4-003422-8.
- Xu, J., Griffin, R. J., Liu, Y., Nakao, S., Cocker, D. R. 2015: Simulated impact of NO_x on SOA formation from oxidation of toluene and m-xylene. *Atmos. Environ.*, **101**, 217–225, <https://doi.org/10.1016/j.atmosenv.2014.11.008>.
- Xu, L., Yang, Z., Tsona, N. T., Wang, X., George, C., Du, L. 2021: Anthropogenic–Biogenic Interactions at Night: Enhanced Formation of Secondary Aerosols and Particulate Nitrogen- and Sulfur-Containing Organics from β-Pinene Oxidation. *Environ. Sci. Technol.*, **55**, 7794–7807, <https://doi.org/10.1021/acs.est.0c07879>.